HAND FORCE AND ARM MOVEMENT COORDINATION IN STATIC AND DYNAMIC MANIPULATION TASKS

A THESIS

Presented to the Department of Mechanical and Aerospace Engineering

California State University, Long Beach

In Partial Fulfillment

of the Requirements for the Degree

Master of Science in Mechanical Engineering

Committee Members:

Panadda Marayong, Ph.D. (Chair)
I-Hung Khoo, Ph.D.
Vennila Krishnan, Ph.D., PT

College Designee:

Hamid Rahai, Ph.D.

By Daniela Herrera

B.S., 2017, California State University, Long Beach

January 2020

ABSTRACT

To be able to interact with the variety of objects an individual encounter with every day, he or she must know how to manipulate those objects. In simple object manipulation, such as the action of drinking a cup of water, the hand force and movement is controlled by the central nervous system (CNS) to regulate the amount of grip force the hand must exert to hold the object without slipping or breaking the cup. However, neurological diseases, such as multiple sclerosis and Parkinson's, affect the function of the CNS causing individuals to lose control of their muscle activation and coordination. There is an extensive set of research dedicated towards investigating the coordination between grip and load force of the hands for a variety of manipulation tasks. However, there is a gap in current research in understanding the relationship between the human hand and the forearm or upper arm movement during object manipulation.

The purpose of this work is to redesign a two degree-of-freedom hand function assessment device that can be used to measure grip force, load force, and arm movements. The new hand function assessment device was used to collect baseline data of five healthy young adults on the coordination between grip force, load force, and arm movement using the elbow angle. Based on the results of the hand function assessment device, elbow angle is not highly coordinated with grip force and load force due to its low coupling and low modulation. A reliability assessment was also conducted to measure the repeatability of the new hand function assessment device by using an intraclass coefficient (ICC) algorithm on the grip force, load force, elbow displacement, elbow lifting speed, and elbow lowering speed. This work ends with a coordination assessment by analyzing each subject's coupling and modulation of grip force, load force, elbow angle and elbow speed. The coordination assessment resulted in the conclusion that the elbow angle is not highly coordinated with grip force and load force. However, upon

making device modifications and collecting more data, the results might show otherwise. After the system is verified to provide repeatable measurements, it can be used to study the coordination of grip force, load force, and elbow angle on a group of individuals with multiple sclerosis.

ACKNOWLEDGMENTS

I would like to give a special thanks to my thesis advisor, Dr. Panadda Marayong, for her continuous support and for allowing me to join her research lab. Dr. Marayong was one of my first instructors in 2013 in an introductory to mechanical engineering course. She was also my instructor for a haptics graduate course that inspired me to purse a thesis. Thank you Dr. Marayong for being flexible with my schedule and for guiding me through the electrical and mechanical design of our hand function assessment device. I also want to say thank you to Dr. I-Hung Khoo, who helped me troubleshoot my circuits many times and helped me print my first prototype circuit board (PCB). Thank you Dr. Vennila Krishnan for helping us review and submit our Institutional Review Board (IRB) application. Thank you, Don Napasindayao, for helping me 3D print parts for the hand function assessment device and for helping me whenever I needed help in the lab. Thank you Ambarish Nayak for helping me jump start into the LabVIEW development. Thank you everyone. I have gained hands on experience and project management skills that have become a valuable asset for me. Lastly, I want to pay a special tribute to my youngest sister, Casandra, for being my biggest motivation on my most challenging days.

TABLE OF CONTENTS

LIST OF TABLES

LIST OF FIGURES

CHAPTER 1

INTRODUCTION

The human hands are essential to fully interact with objects people come across in their day-to-day lives. Not only do hands support a wide range of tasks, such as holding, gripping, and lifting, they are also the organ with the most mechanoreceptors. Object hand manipulation tasks can be static or dynamic. An example of a static task is when an individual uses the hand rail of a bus, in order to get inside of the bus. The rail does not move and is mounted on the side of the entrance of the bus, so the individual uses it as support and grips onto the rail accordingly to not fall. An example of a dynamic task can be when an individual works out and uses dumbbells to gain bicep muscles. Depending on the weight of the dumbbells, the individual must carefully adjust their grip, when lifting the dumbbell. This task is dynamic because the dumbbell moves with the individual. There are also unimanual and bimanual object manipulation tasks. Unimanual simply describes a task with the use of one hand one, like changing the channel of the tv with a remote. While bimanual describes tasks that require two hands, such as lifting a box from the ground. Due to the wide range in types of manipulation tasks, hand function has been of primary interest in research and has provided very useful studies to support what defines good coordination of the hand.

There are studies that have been done in the past that focus on the coordination between grip force and load force and help define the differences between high and low coordination. Experiments have been conducted to explore the differences between groups of healthy individuals and groups with neurological disease that have deterioration of their hand function. Research has proven that high coordination of grip force and load force is due to stable grip-to-load ratios, high force coupling, and high grip force modulation [2,4]. Although there is

promising work of the coordination between grip force and load force, research lacks studies on the role of arm movement, such as arm angle and lifting speed, in relation to the hand forces.

The first motivation behind this work is the re-design of a unimanual two degree of freedom hand function assessment device, that was previously used to only measure grip force and load force. The goal behind the re-design of the new device was to transform into a three degree of freedom device that also measured and monitored arm movement. The modified device consists of two load cells, an accelerometer, and a goniometer. Another major modification between devices is the new capability to use the hand function assessment device for static and dynamic manipulation tasks. The previous device was designed to be used for dynamic testing only.

The second motivation behind this work was to collect baseline data on a group of healthy subjects. After building the new device, it was used to start the investigation in research to provide a coordination assessment for hand forces and arm movements. For each subject in the group, grip force, load force, and elbow angle were monitored and collected throughout each experiment by using the modified device in junction with a LabVIEW graphical user interface. Data analysis methods were developed to post process the sensor measurements and determine the relationships between hand forces and arm movement parameters.

This work begins with a literature review of prior work conducted on hand force coordination. Then, this work provides an overview of the hand function assessment device by describing the mechanical design, sensor integration, LabVIEW graphical user interface, and the circuit design that were implemented in the re-design. After, the sensor calibration and conversion methods are listed in the following system validation chapter. Then, a user study is presented with a discussion of the subjects recruited, the experimental protocol, and the

collection of baseline data. This work follows the user study chapter, with a discussion of the results obtained from subject experiments and an analysis on the baseline data. This work ends with the final conclusions withdrawn from analysis and lists recommendations for future work.

CHAPTER 2

PRIOR WORK ON HAND FORCE COORDINATION

A range of research papers, concentrated on the study of hand impairment, were used as the technical foundation for this work. Research was focused on force coordination in unimanual hand object manipulation for static and dynamic tasking. Unimanual tasks involve the usage of one hand only, while bi-manual tasks involve both. An example of a simple static task is the action of pulling on a stair handrail for support while walking down a flight of stairs. A simple dynamic task can be represented by the action of picking up a water bottle from a table, drinking water from it, then setting it back down on the table from which is was picked up. Both of these tasks are examples of daily unimanual object manipulation tasks.

The two forces that have been studied in literature are grip force (G) and load force (L). Such literature focused on the coordination between grip force and load force. These forces will be defined in this work with the help of the force coordination schematic in FIGURE 1. . Below, the rectangle represents an ordinary everyday object and the ovals represent fingers and a thumb in contact with that object. Grip force is the force applied normal to the contact area of the fingers and thumb when holding or pulling on an object. Load force is the force applied due to the weight of an object, is tangential to grip force and is in the direction of gravity. Friction force is applied by increasing the grip force on the object to prevent slippage, which is consequently caused by load force [1]. In Figure 1, grip force is abbreviated as GF, load force is abbreviated at LF, and friction force as FR. In this work, G and L are used for simplicity.

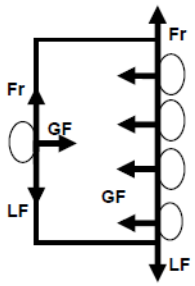

FIGURE 1. Force coordination schematic [1].

G/L ratio, force coupling, and grip load (G) modulation are variables that are used for assessment in research and clinics where hand function is studied and evaluated for patients with neurological diseases. G/L ratio describes the amount of grip load that was used to prevent slippage and its value brings insight to help distinct good from poor force coordination. The level of force coupling in force coordination is assessed by the correlation coefficient for such forces and the time lag between them. Grip load modulation is derived from the slope and intercept in the regression lines of grip force and load force plots (G vs. L). In literature, the slope in such regression equations is referred to a gain and the intercept is referred to as the offset in grip force modulation [1-3].

As previously mentioned, force coordination has been assessed by evaluating an individual's G/L ratio, G modulation, and force coupling. High force coordination has proven to be a result of a stable G/L ratio, high force coupling (high correlation coefficient and low time lags between G and L), and high G modulation (high gain or low offset or both from regression plots) [2,4]. Individuals who suffer from neurological diseases such as Parkinson's disease, Huntington's disease, cerebellar lesions, cerebellar atrophy, stroke, or multiple sclerosis, typically experience a deterioration in force coordination. Such individuals experience an elevated G/L ratio, low force coupling, and low G modulation. An elevated G/L ratio could cause

a person to get tired quickly, and over grip hand-held object [4,5]. Other individuals that suffer from a degrading force coordination are those that have any part of their hand anesthetized since the hand is a highly concentrated receptor organ. Skin receptors play an important role in sending sensory information to the central nervous system (CNS) [1,6].

In a study, in which a group of individuals with mildly multiple sclerosis (MS) and a group of healthy individuals (HC) participated, an experiment was conducted to compare the force coordination between the two groups during manipulation tasks [2]. The results for that study are displayed in Figure 2 and was included in this study to help illustrate the distinction between high and low force coordination. The G/L ratios, correlation coefficients, time lags, gains, and offsets are plotted and compared for both groups of subjects (MS vs. HC). Each subject was tested on three different tasks. There were two dynamic tasks (referred to as "Lift" and "Oscillation" in Figure 2) and one static test (referred to as "Ramp" in Figure 2). As it can be seen in the figure below, regardless on which type of test was conducted, MS subjects experienced higher levels of G/L ratios when compared to the HS patients. Also, there was much more variability in the MS patient data for the correlation coefficient, time lag and gains. HC patient data mainly resulted in consistent high correlation coefficients, time lag, and gains. Also, HC patient offsets were lower than those for MS patients. Most of the results in this experiment found in literature agree with the distinction between high and low force coordination described in previous paragraphs.

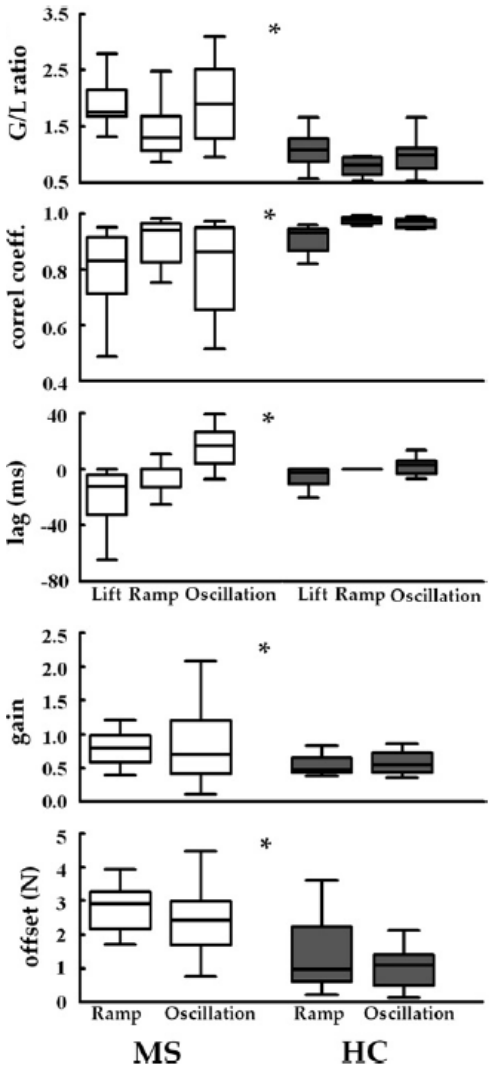

FIGURE 2. Example of force coordination comparison between a group of individuals that suffer from mildly multiple sclerosis and a healthy controlled group [2].

Change in direction and hand dominance also play a role in force coordination of the human hand. A bidirectional task, such as shaking an object, is performed by applying a load force in two opposite directions. A unidirectional task is only performed in one direction, such as only pushing or only pulling on an object. A study has shown that when changing from a unidirectional task to a bidirectional task, there can be in increase in the G/L ratio and a decrease in force coupling and G modulation [4]. Such results are supported by evaluating the simplicity or complexity of the two tasks (unidirectional and bidirectional). A unidirectional task is simple

and only requires a stable muscle synergy to carry on the task, while the bidirectional task requires a constant switching of two distinct synergies. Constantly switching directions, especially at a rapid rate, deteriorates force coordination and makes the task much more complex than a unidirectional task [4]. Literature also supports the role of hand dominance in force coordination. Experiments have been conducted to explore the distinction in task performance between the dominant and non-dominant hand. Throughout experimentation, it has been concluded that the non-dominant hand tends to experience higher levels of grip force modulation. Also, interestingly enough, it was also discovered that the non-dominant hand is better at controlling the direction of load force than the dominant hand [4].

Although literature has contributed largely in force coordination of hand function, there is a gap in research in regards to the effect of arm movement. This work focuses on exploring the contribution elbow coordination brings during unimanual manipulation tasks. With the collection of baseline data, there is new insight on how elbow angle and movement speed play an influence grip and load force of the hand.

CHAPTER 3

HAND FUNCTION ASSESSMENT DEVICE OVERVIEW

In 2018, a two degree-of-freedom training device was developed to study grip and load force coordination [7]**.** The system consists of an accelerometer, a load cell with an amplifier, an Arduino, force plates, a hand cup body, and an electronics chassis as shown in Figure 3 below. The accelerometer was used to calculate the load force created by the weight of the device and the load cell was used to calculate the grip force applied by a user gripping the force plates on the sides of the hand cup body. The Arduino was used to collect sensor data and was stored inside of the electronics chassis, along with the sensors. This device was used to assess hand impairment in unimanual (one-hand) and bimanual (two-hand) manipulation tasks. A user interface was also developed to provide visual feedback, plot force correlation, and display their corresponding delay.

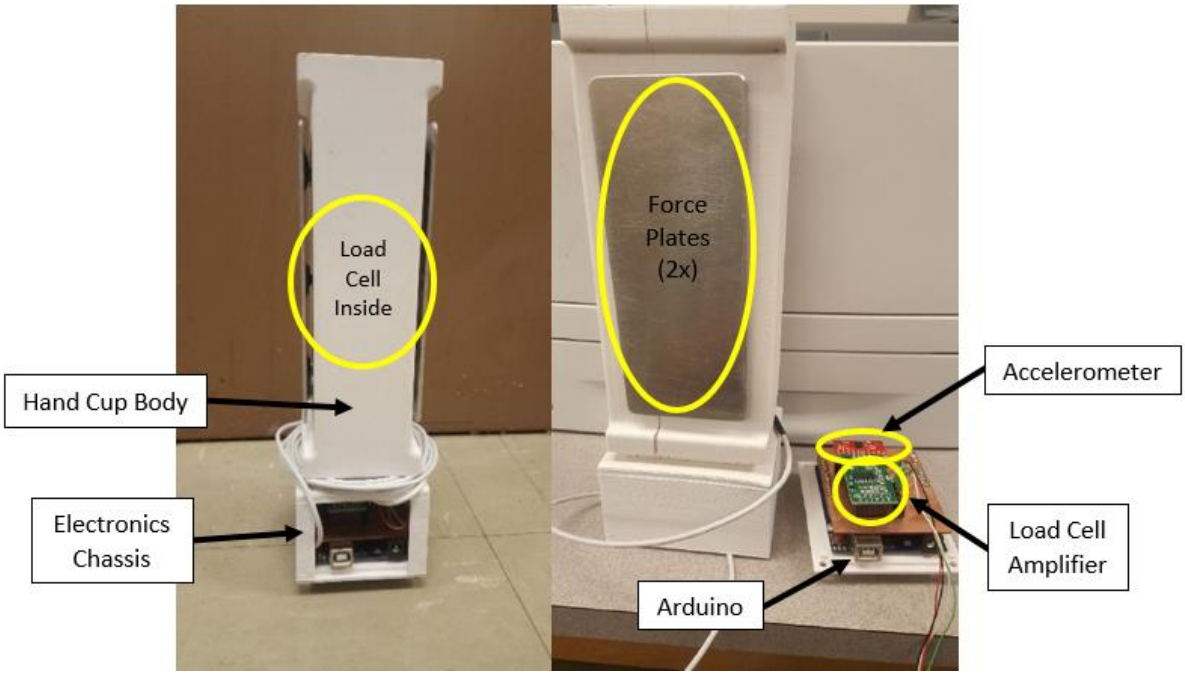

FIGURE 3. Two degree of freedom design front (left) and side (right) profiles [7].

In this work, a goniometer was added to the existing design to measure the elbow angle for the purposes of studying grip and load forces and arm movement coordination. One of the main differences between designs is that the previous design was only used for dynamic testing and was not set up for static testing. For the modified design, it was necessary to add a second load cell specifically for measuring the grip force during static tasks. In addition, the new design includes a compartment for additional weights that can be added as an experimental condition for dynamic tasks. The printed circuit board used in the old design was modified to include the integrated circuit for the goniometer and static load cell, which requires a redesign of the electronics chassis.

The modified design was used to collect grip force, load force, and elbow angle on a group of healthy individuals to generate a baseline data set for future studies with subjects with hand impairment. By having elbow angle available, it was also possible to derive the lifting speed and lowering speeds during dynamic testing. During static testing, the device was mounted onto a vise to keep it from moving and inclined at 5° for subject comfort. As shown in Figure 4, the electronics chassis, which is the lower half of the device, was bolted onto an adapter. The two yellow adapters in Figure 4 secure the Futek load cell in place, to avoid rotation of the device and keep the device static. The Futek load cell will be described in more detail in the sensors section of this chapter. In the static configuration, the device measured the pulling force and elbow movement of a subject. During dynamic testing, the device was removed from the adapter, but was still kept on top of it to keep the device at the same level as in the static scenario.

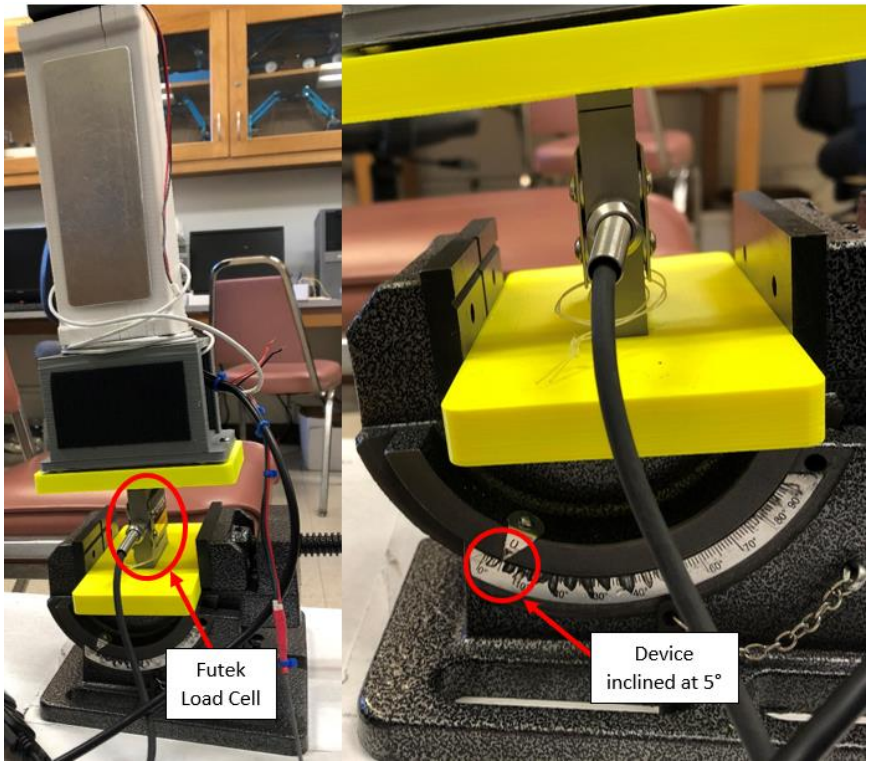

FIGURE 4. Modified hand function assessment device with an adaptor for static test.

To collect sensor data for a subject's grip force, load force, and elbow angle, it was necessary to add additional components to older training device and it was also necessary to make electrical and mechanical modifications. The redesign of this device was required to accommodate static and dynamic tests, which consisted of simple pulling and lifting manipulation tasks. A more detailed description of each test scenario will be later discussed in the User Study chapter. The following sections discuss the mechanical design, sensor integration, the LabVIEW interface that was develop to collect data, and the circuit that was built.

3.1 Mechanical Design

The mechanical design for the device was carried over from the previous design with a few modifications. Both the static and dynamic configuration include a hand cup body piece (which was not modified from the previous design). The old electronics chassis was modified to

fit the new and larger printed circuit board and it was also designed in a way such to facilitate test switching, from static to dynamic or vice versa. The hand cup body is attached to two force plates which add a compressive load to the Omega load cell when gripped by a subject. Figure 5 shows where the Omega load cell is placed inside of the hand cup body.

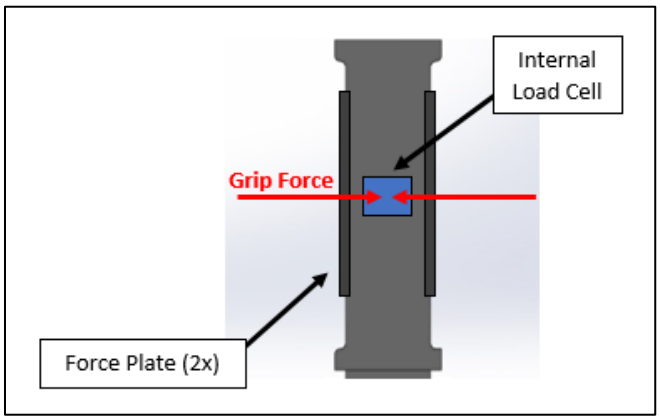

FIGURE 5. Hand cup body side profile.

The design goal for the static configuration was to have the ability to fix the hand function assessment device and to measure a tension load applied purely in the z-direction. For that reason, two plates were designed to fix the Futek load cell from rotating and also to avoid sensor damage when mounted on a vise. Figure 6 displays the Solidworks model that captures the configuration for static testing. For the dynamic configuration, shown in Figure 7, it was desired to capture an individual's motion when lifting the device with two different masses. The first mass was composed of only the hand function assessment device with the electronics chassis which weighed 800 grams. The second mass was composed of the hand function assessment device, the electronics chassis, the weight compartment and circular disks. The weight compartment was designed to carry nine circular disks that each weighed 50 grams as shown in Figure 8. The weight compartment with the circular disks weighed 515 grams, which totaled a 1315 grams overall weight for the second mass. The purpose for varying the device's

mass during dynamic testing, was to evaluate the changes and correlation in elbow movement during the lifting and holding phases.

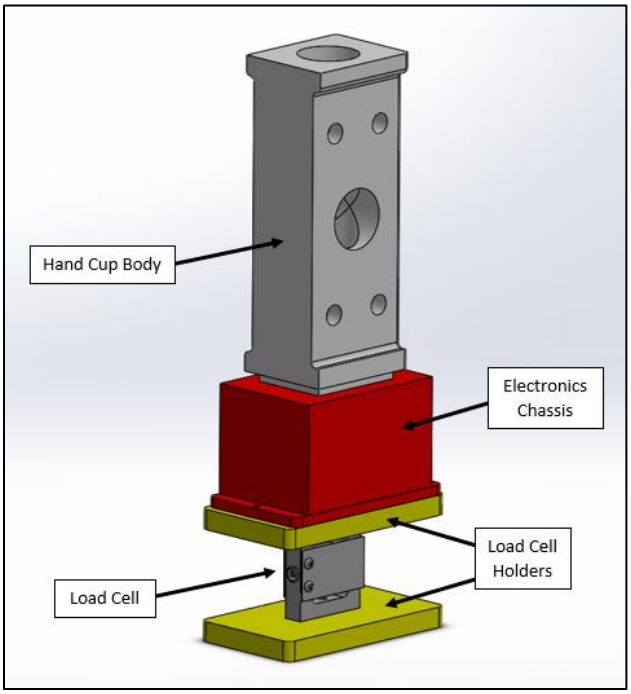

FIGURE 6. Static configuration mechanical design overview.

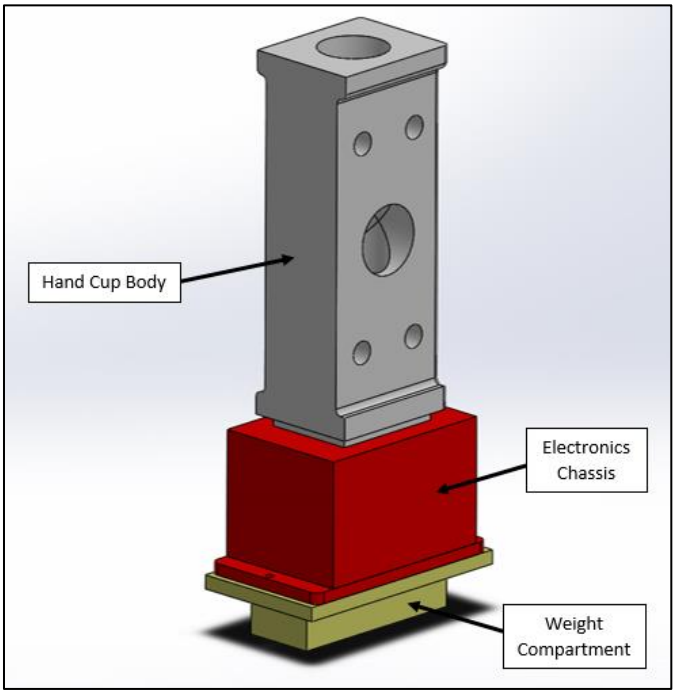

FIGURE 7. Dynamic configuration mechanical design overview.

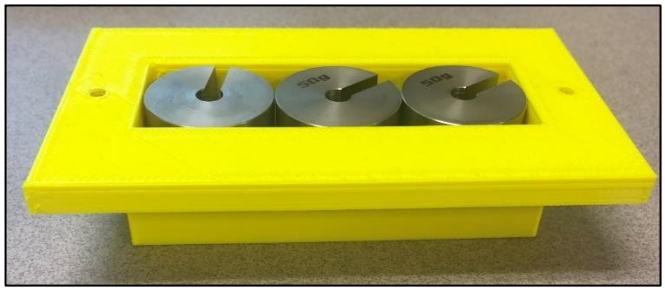

FIGURE 8. Weight compartment with 450g of additional mass.

3.2 Sensors Integration

The older device consists of two main sensors, a load cell and accelerometer. The accelerometer was kept and was used during dynamic testing to capture a subject's hand and elbow motion. The Omega load cell was also kept to capture grip force during both static and dynamic testing for the new device. In the following paragraphs, each sensor used, including the ones from the previous design, are discussed.

To measure the grip force of an individual, the Omega load cell that was used from the previous design, was used for the new design. This load cell was attached to two force plates that were placed on the opposite sides of the device. The load cell is capable of measuring tension and compression loads, but only compression loads were used for this study. In conjunction, a HX711 amplifier was used due to the load cell's small signals and its resolution [7]. Figure 9 shows the grip sensor that was used inside of the device.

To measure load force for two distinct tasks, two different sensors were used. The previous design used an MPU-6050 Triple Axis Breakout Board to measure the acceleration of a user. The same acceleration breakout board was used to calculate the load force during the dynamic manipulation task. The accelerometer was placed inside of the electronics chassis on the printed circuit board. For the static manipulation task, a Futek load cell was used to measure a

subject's pulling force. Due to the size of the load cell, the Futek sensor was placed outside of the device and fixed on a mounting vice to keep the device from moving or rotating. A Futek amplifier was used to increase the Futek load cell's signal before inputting the signal into the Arduino. A power supply of 4 AA batteries and voltage regulator were used in junction to feed the Futek amplifier and load cell with a required excitation voltage of 10 VDC. Both of the sensors used to calculate load force can be seen in Figure 9.

In the previous design, the device did not have a sensor to measure elbow angle. Since elbow angle was of particular interest for this study, a Biometrics twin axis goniometer was added to the device to provide that measurement. The measurement of the elbow angle also provided insight of a subject's lifting and lower speed during dynamic testing. For the present study, only one axis was used to capture a subject's elbow flexion throughout the manipulation tasks. An individual was not expected to bend their elbow more than 90° for either the static or dynamic manipulation task. The goniometer was powered by an Arduino since it required minimal power. Since the output of the goniometer was too low in value for an Arduino to read, an operational amplifier was used to increase its value. The goniometer was secured to the subject's forearm and upper arm with athletes' tape and was calibrated before each session. The goniometer used for this study is shown in Figure 9.

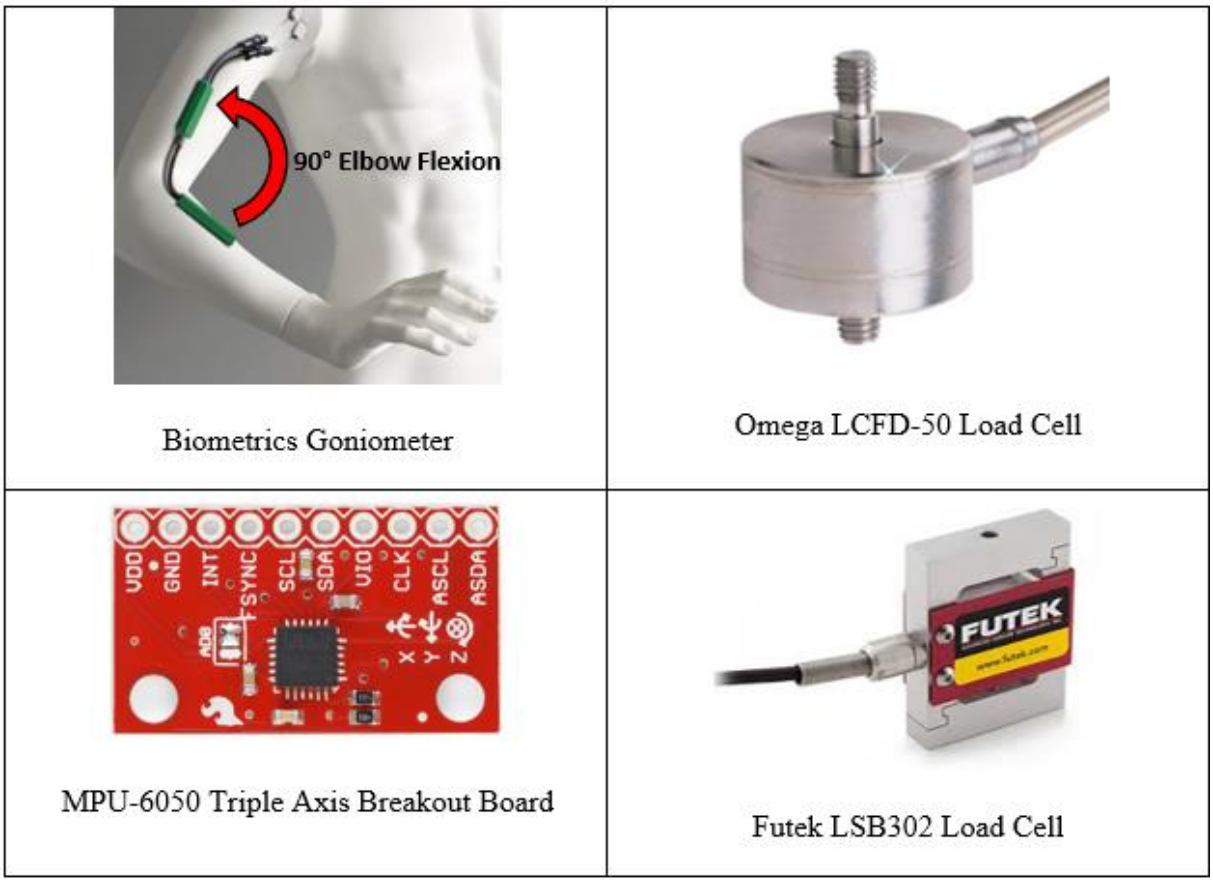

FIGURE 9. Sensor matrix.

3.3 Graphical User Interface using LabVIEW Virtual Instrument

To monitor the data real time, a virtual instrument was created in LabVIEW. It was necessary to develop event driven scenarios to allow calibration for each session, selection of static or dynamic test, enter user information (hand in test, subject code, etc.) and to have the ability to save the data to a text file for further analysis. Figure 10 shows a flow diagram of the virtual instrument's event sequence. After sensor calibration, the virtual instrument kept track of the sensors' offsets for later use. Once a static or dynamic test was initiated, sensor data was read from an Arduino as a string at a rate of 20 Hz. Since the string contained the value of every sensor, separated by commas, the string was then split into individual values. The offsets that

were previously recorded from calibration were then subtracted from the raw values of each sensor. Then, the raw values were converted to the appropriate unit of Newtons for load force and grip force or degrees for elbow angle. After unit conversion, the load force, grip force and elbow angle were plotted in real time and saved to a text file for later analysis. Figure 11 shows an example of data being plotted by the virtual instrument during a dynamic scenario without weights involved.

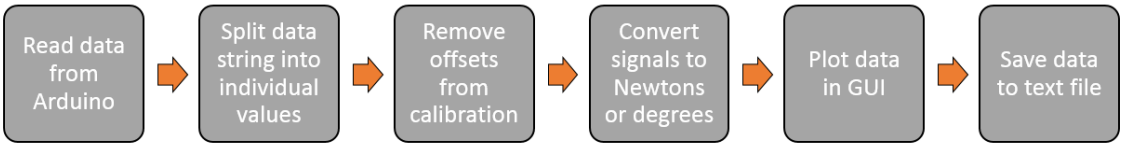

FIGURE 10. LabVIEW virtual instrument flow diagram.

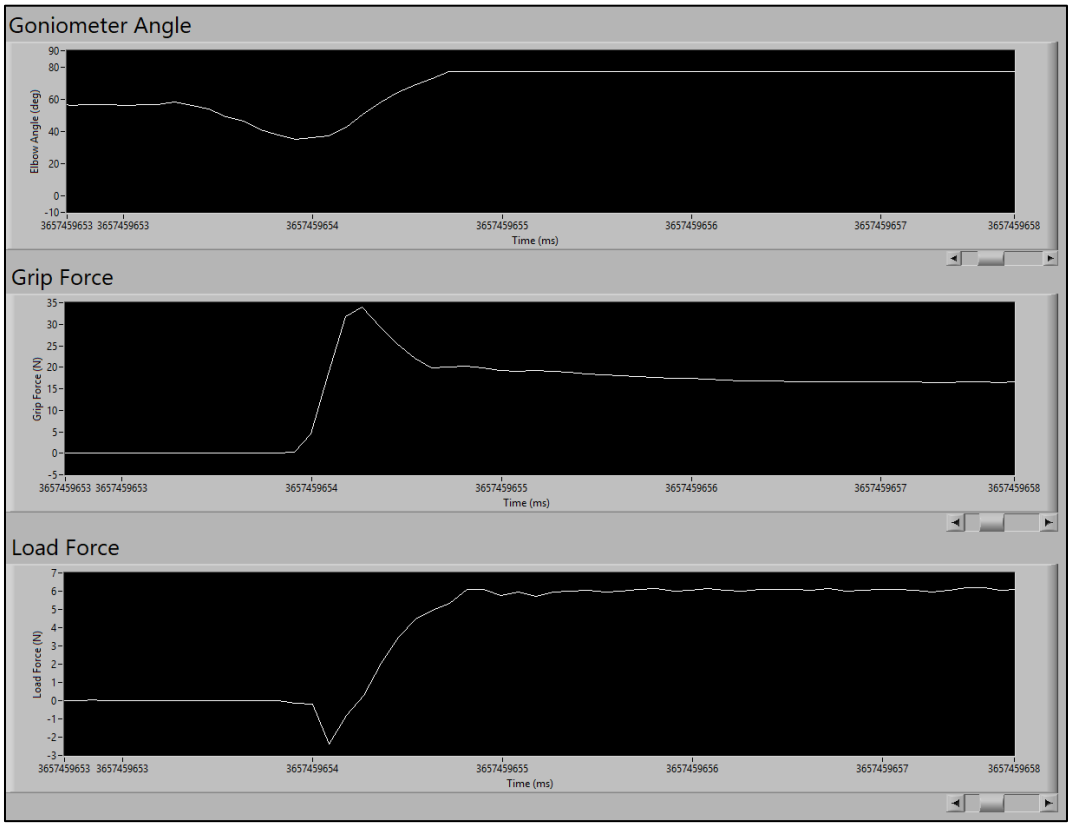

FIGURE 11. LabVIEW GUI plots for a single patient during dynamic testing with no weights.

3.4 Circuit Design

A printed circuit board (PCB) was selected to layout sensor pins and modules compactly to fit inside the electronics chassis, inspired by the previous design. The board was designed using the free EAGLE PCB design software and then the board was printed in the Electrical Engineering Department in CSULB. Figure 12 shows an overview of the printed circuit board with all of the electrical components and header pins on it and Appendix A displays snapshots of the EAGLE schematic and board layout.

As it can be seen in Figure 12, the PCB was design in such a way to fit as a "mother board" for an Arduino. The two outer lines of header pins connect to every digital and analog Arduino pin, as well as its power pins perfectly. The HX711 load cell breakout board was used to amplify the output of the Omega load cell and the XL6009 voltage regulator was used to shift the input power for the Futek load cell as they were described in the previous section. The PCB was designed to be easily modifiable and to give future users the ability to connect additional sensors to the circuit.

Figure 13 and 14 display the static and dynamic configurations for the electronics that were used in those scenarios. For static testing, the Futek load cell, goniometer and Omega load cell were used. For dynamic testing, the MPU 6050 accelerator, goniometer, and Omega load cell were used. The raw sensor measurements were captured and displayed for the operator using the LabVIEW Virtual Instrument. The following chapter will cover the sensor calibration and unit conversion done by the virtual instrument in the System Validation chapter.

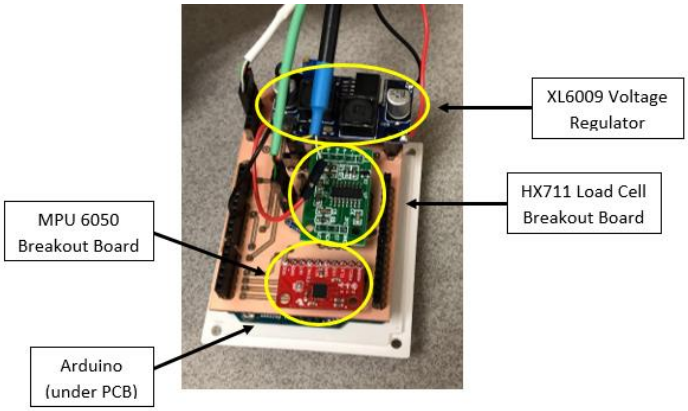

FIGURE 12. PCB layout.

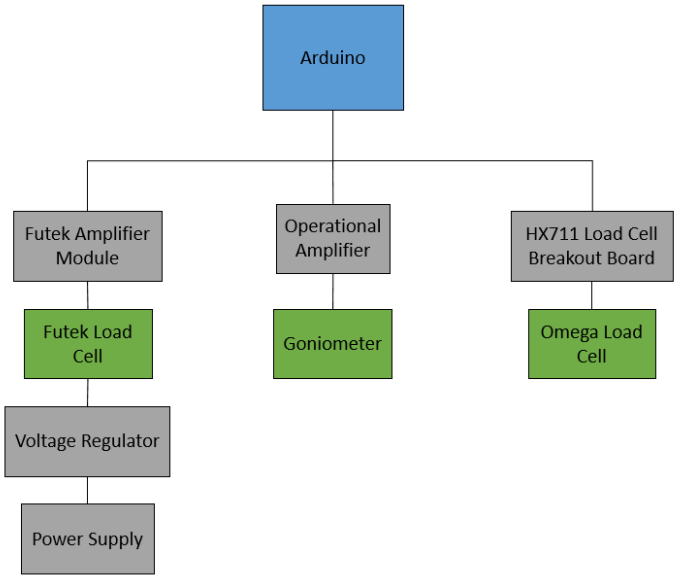

FIGURE 13. Static test electronics configuration.

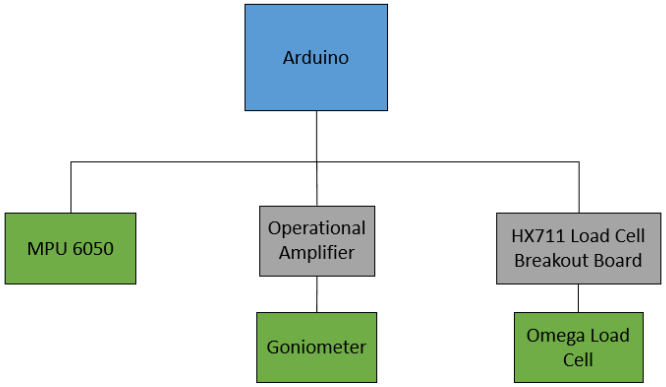

FIGURE 14. Dynamic test electronics configuration.

CHAPTER 4

SYSTEM VALIDATION

To ensure proper sensor readings, each sensor was carefully tested and calibrated. As part of the calibration procedure, the goniometer and Futek load cell were tested at different angular displacements and loads to validate sensor outputs. The Omega load cell and accelerometer were previously tested during the first design of the device and were not retested during the redesign of the device. The following sections include a detailed description of the sensor calibration testing, the internal LabVIEW calibration process, and the sensor output conversion to elbow angle, load force, and grip force.

4.1 Sensor Calibration Testing

As mentioned in the preceding paragraph, the goniometer was tested at different angles to capture its output voltage range. The Biometrics goniometer used for this experiment was attached to a digital goniometer as shown in Figure 15. The accuracy of the angles measured by the Biometrics goniometer were checked by verifying the values on the digital goniometer. The goniometers analog pins were attached to an Arduino and their values were displayed on a computer screen. Voltage values were collected on an Excel spreadsheet for the angular range of -120° to 120° in increments of 5°. The calibration data for the goniometer can be found in Appendix B. Below, Figure 16 graphically displays the results for the goniometer calibration data. The goniometer angle and voltage output appeared to have a linear relationship, which made data conversion easy to handle during experimentation.

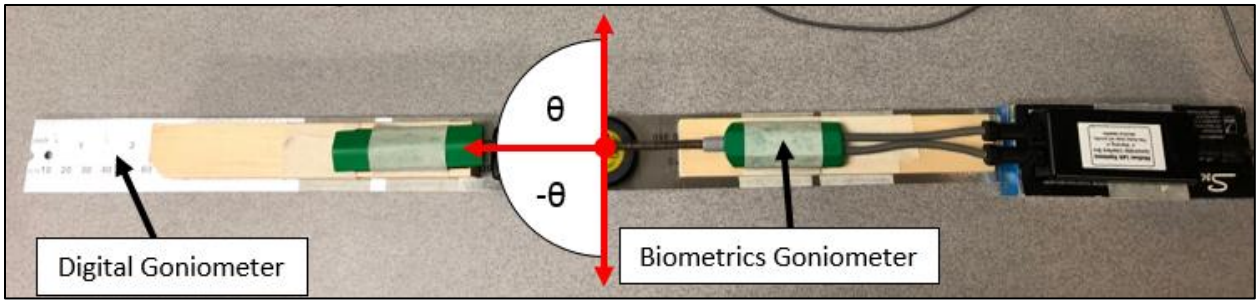

FIGURE 15. Goniometer calibration setup at 0°.

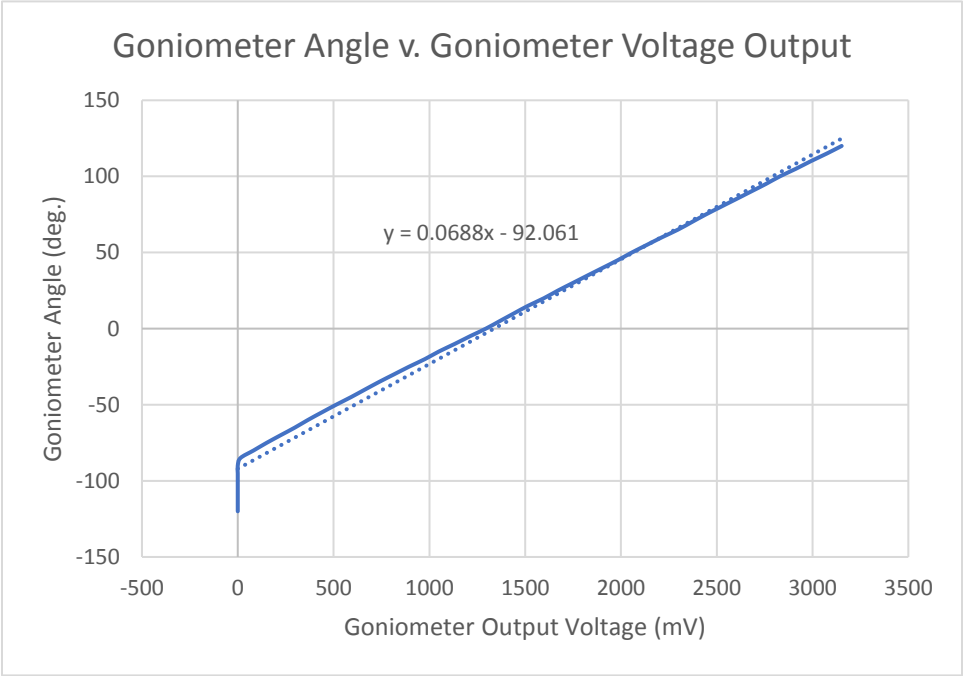

FIGURE 16. Goniometer calibration data.

The Futek load cell was also tested at different loads during its calibration process. The Futek load cell was mounted onto a stable structure with a carabiner keychain secured on its opposite end. The Futek load cell used has a capacity of 50 lb., however, it was not necessary to test the sensor to that load capacity for this experiment. A combination of different loads up to 18.331 lb. were carefully applied and supported by the carabiner keychain as shown in Figure 17. In a second Excel spreadsheet, the load cell's output voltage was recorded for each load applied.

The calibration data was then plotted to gain insight on the relationship between output voltage and load. As observed in the previous case, Figure 18 also displays a linear relationship and also made it relatively easy to convert load (weight) to load force. The LabVIEW internal calibration is briefly discussed in the following section.

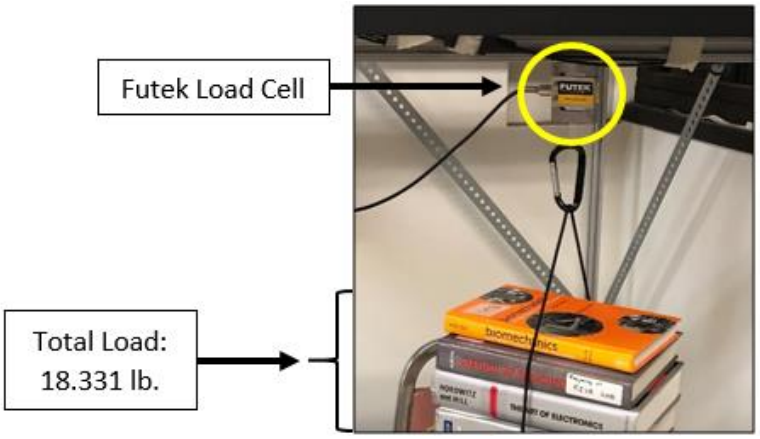

FIGURE 17. Futek load cell calibration setup.

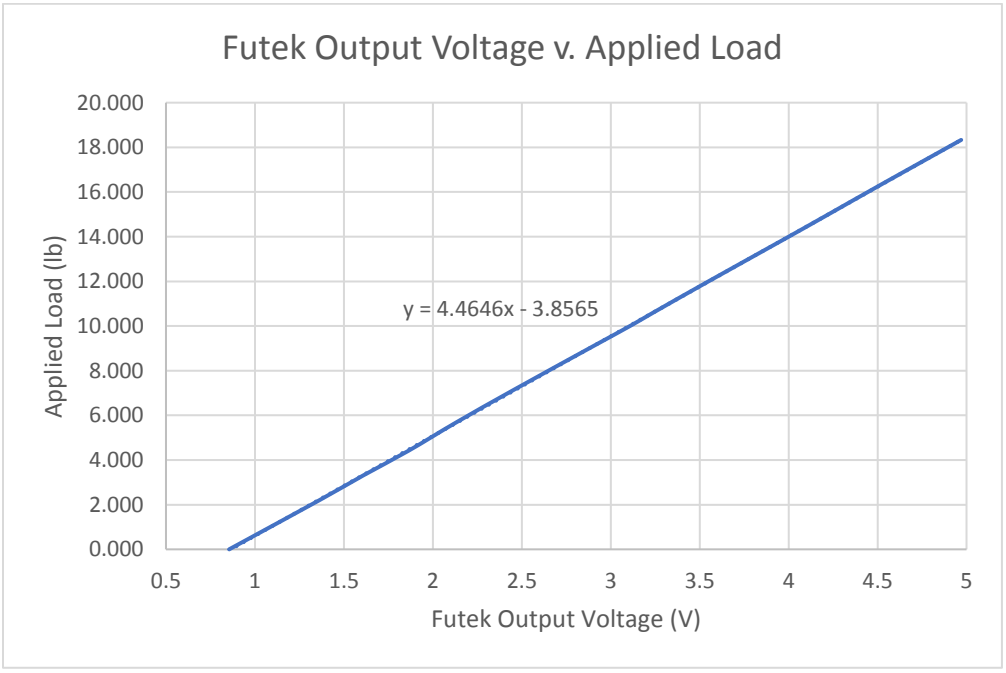

FIGURE 18. Futek load cell calibration data.

4.2 Sensor Output Conversion

Sensor conversions were generated based on the previous calibration testing and their output. The conversions for each sensor are summarized in Figure 19.The goniometer outputs an output voltage, and after the removal of its offset, it is converted into elbow angle. To convert the output voltage into elbow angle, the virtual instrument used the linear equation found when testing the goniometer independently as discussed in section 4.1. Equation (1) is the linear equation that was used to interpolate and find the elbow angle when given an output voltage from the goniometer.

$$\theta_e = 0.0688V_g - 92.061, \tag{1}$$

where θ_e is the elbow angle in degrees and V_g is the goniometer voltage reading in mV.

The static load force was found using a similar method as like for the goniometer. The Futek load cell outputs an output voltage which was converted into applied load, in pounds, using interpolation with Equation (2). The interpolation equation used in this step was generated from independent Futek sensor testing as discussed in section 4.1. The applied load is then converted from pounds to kilograms (Equation (3)), and is lastly multiplied by gravity to determine the load force applied during static testing (Equation (4)).

$$W_{lb} = 4.4646V_{FL} - 3.8565, \tag{2}$$

where W_{lb} is the applied load in lb. and V_{FL} is the Futek load cell output in V.

$$W_{kg} = 0.4536W_{lb}, \tag{3}$$

where W_{kg} is the applied load in kg.

$$L_s = gW_{kg}, \tag{4}$$

where L_s is the static load force in N and g is gravity in m/s^2.

The dynamic load force was calculated differently than the static load force because of the use of different sensors. A load cell was used to calculate the load force for static testing and an accelerometer was used for dynamic testing. The raw accelerometer readings were multiplied by 2048, which was the recommended unit g per the datasheet of the sensor (Equation (5)). Then, the new acceleration value was divided by the weight of the object by using Equation 6. Since dynamic testing was comprised of two cases, one with weights and one without, the weight of the device was adjusted by the virtual instrument accordingly.

$$a_{adj} = \frac{a_{raw}}{2048}, \tag{5}$$

where a_{adj} is the adjusted acceleration output in m/s^2 and a_{raw} is the raw acceleration output in m/s^2.

$$L_d = W_d a_{adj}, \tag{6}$$

where W_d is the weight of the device in kg and L_d is the dynamic load force in N.

Lastly, the output for the Omega load cell was converted to grip force applied by a subject. An Arduino module was used to convert the voltage output of the Omega sensor into grams by using an internal function, before getting read by the virtual instrument. Once the virtual instrument had access to this value, it divided the grams output by 1000 to convert it to kilograms using Equation (7). Afterwards, the kilograms output of the Omega sensor was multiplied by gravity to get converted in grip force in Newtons (Equation (8)).

$$O_{kg} = \frac{O_g}{1000}, \tag{7}$$

where O_{kg} is the Omega load cell output in kg and O_g is the Omega load cell output in g.

$$G = gO_{kg}, \tag{8}$$

where G is the grip force in N.

The virtual instrument was not only used to collect raw sensor values and monitor experimental data, but was also very useful when calibrating each sensor. The internal calibration process was conducted at the beginning of each trial, but can be modified to calibrate only once during a session period. Making this modification to the virtual instrument, will make it more rigid, optimal, and will allow for more time for additional test scenarios.

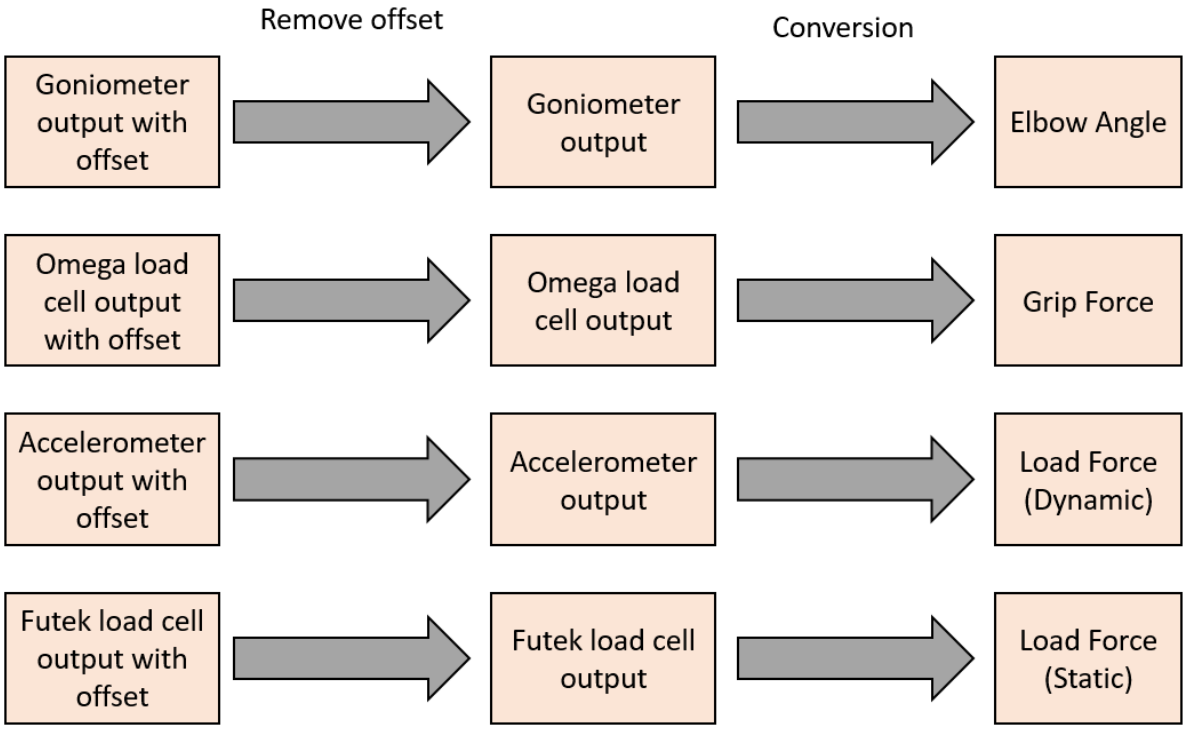

FIGURE 19. Sensor output conversion.

4.3 LabVIEW Internal Calibration

After each sensor was testing and their outputs validated, the sensors were ready for testing. At the start of each trial, a subject was asked to extend their arm, with the goniometer attached, in order to capture an elbow angular reading of 0° by the LabVIEW virtual instrument. Figure 20 shows a subject with their arm extended during the LabVIEW calibration procedure. The values of the load cells and accelerometer were also captured in static position during this internal calibration. The virtual instrumented collected data at 20 Hz for three seconds and then took the average of each sensors' output during static operations. By obtaining these averages, the virtual instrument had the ability to calculate and remove offsets to ensure repeatability of the experiment. The sensor conversions for each sensor are discussed in the following section.

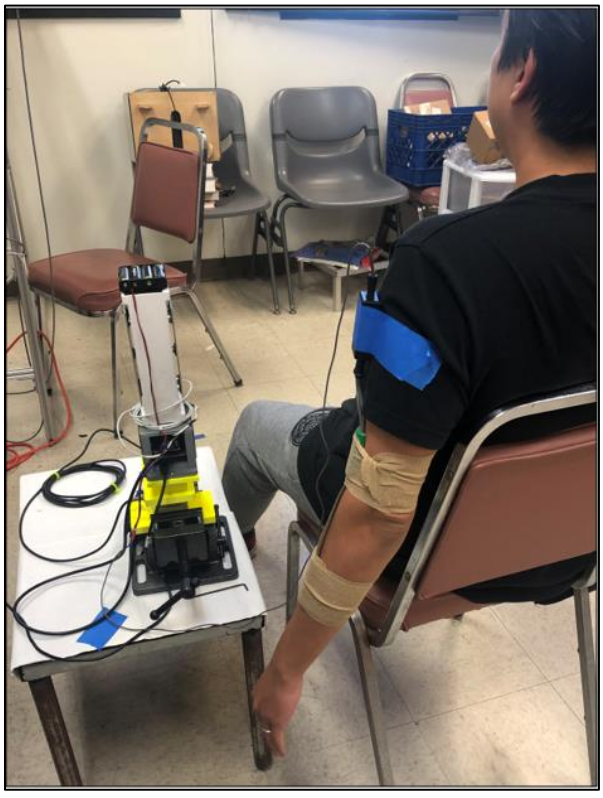

FIGURE 20. Subject during calibration procedure.

CHAPTER 5

USER STUDY

To further validate system reliability, a study on the coordination of hand forces and arm, was conducted on a group of five healthy subjects. The study consisted of collecting baseline data for individuals with high coordination for grip force, load force, and elbow angle. Literature describes high coordination between grip force and load force by and individual having a stable G/L ratio, high force coupling (high correlation coefficients and low time lags), and high grip force modulation (high gain and low offset from regression lines) [5]. Elbow angle was measured and studied to evaluate its relationship to high force coordination during static and dynamic manipulation tasks. The following sections will further describe the individuals that were part of the study, the experimental protocol and how the baseline data was collected. The experiment was approved by the California State University, Long Beach Institutional Review Board.

5.1 Subjects

Five healthy young adults were recruited to participate in this study based on a subject inclusion/exclusion questionnaire survey. The inclusion/exclusion criteria consisted for healthy subjects are the following requirements: (1) must be aged between 21-30 years of age, (2) capable of independent living, and (3) must have normal or corrected to normal vision. The group of subjects consisted of two females and three males that were between the ages of 21-27 years. Every subject was right hand dominant and did not have any history of medical illnesses or conditions. To protect personal information, each subject was assigned an identification number that was used to reference each person during data analysis.

5.2 Experimental Protocol

On the day of the data collection, the experimental procedures, risks and benefits were once again explained to each subject. The subject was given the chance to ask questions before signing and submitting the consent form. Then, each subject read and signed the consent form and was emailed their form for personal records. The protocol consisted of measuring the maximum grip force and conducting a static test and two dynamic tests for each hand separately. Each test case was conducted five times and then the average was taken for data analysis. The experiment was repeated twice, with a week in between to validate system reliability. With two testing sessions for each subject, the total duration for each experiment was 1-2 hours. The subject was also allowed practice time before starting the first session. Subjects were asked to wash their hands and wipe their hands dry to prevent slippage caused from sweat or any other residue from previous activities.

Subjects were then asked to sit in the subject's chair and were also asked to adjust themselves in a position where they found themselves able to naturally and comfortably pick up the device. Figure 21 shows the experimental setup once the subject sat next to the device. Although not displayed in Figure 21, the computer used for testing was always turned away from the subject to avoid distraction during the data collection. Visual feedback was not part of this study.

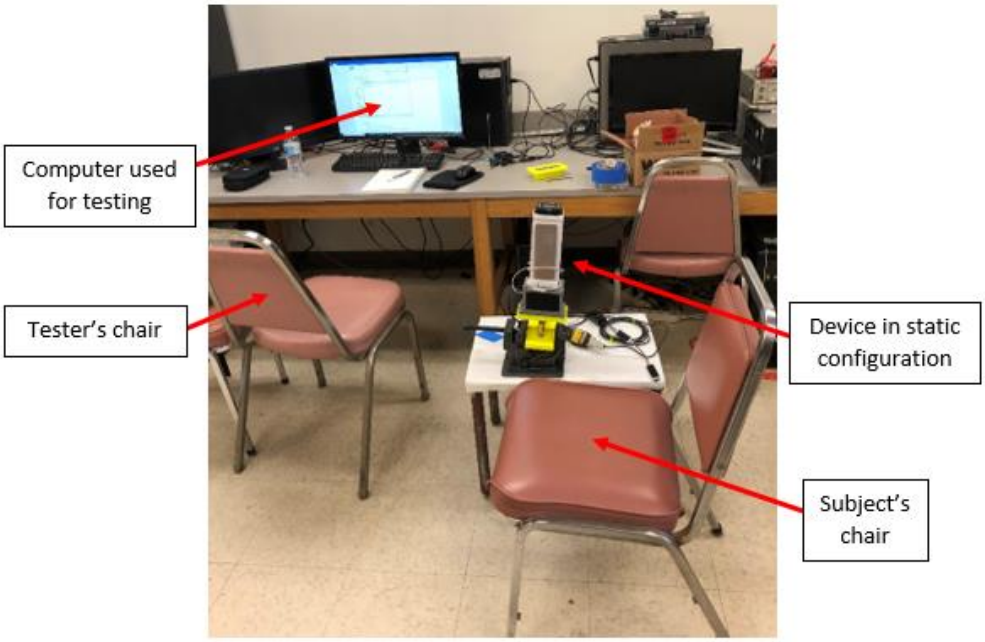

FIGURE 21. Experiment setup.

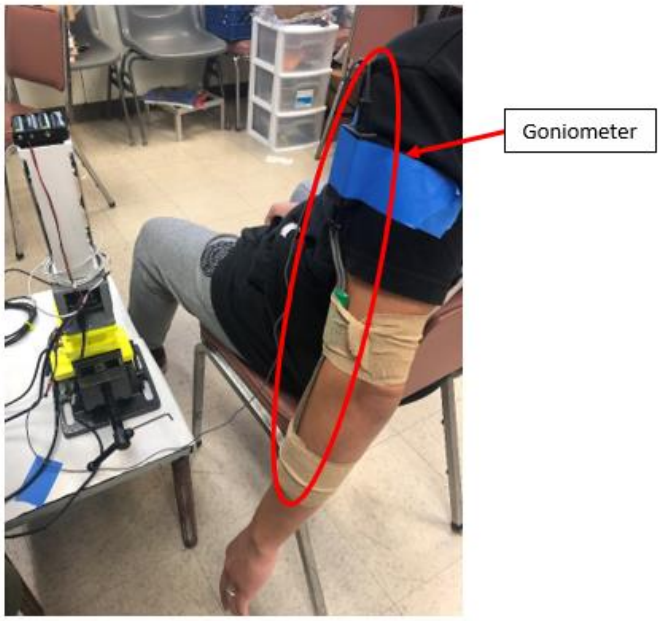

FIGURE 22. Goniometer attachment on subject.

Once each subject had found their optimal sitting position, the goniometer was attached to their arm using athletes' tape. Figure 22 displays how the goniometer was attached to each

subject. The experiment began with testing of the right hand first, then the experiment was repeated on the left hand. The LabVIEW virtual instrument that was used to collect data was programmed to beep three times, with a delay of 3500 milliseconds in between each beep. The beeps provided by the virtual instrument were used to instruct the subject to perform a specific action. The actions that were performed were unique to each test case scenario.

Each experiment started with taking a measurement of a subject's maximum grip. For this test case, the device was fixed in the static configuration without any weights. This was a pre-test to the experiment's main testing, but the virtual instrument was still utilized. Once this test case had commenced, the subject was asked to extend their arm and hold in the calibration position to calibrate the sensors. Then, the subject was asked to move their hand towards the device and be ready to grip as how as they could, without hurting themselves. Then, the subject was asked to grip the device each they heard a beep from the computer for about a second. After taking this measurement, the experiment continued with the static test case.

The device was kept in the static configuration and subjects were reminded on the actions they were to perform. For the static test, subjects were first instructed to go to the calibrate position for sensor calibration and then after, go to the rest position and be ready to act on each beep. The resting position was set up to be a comfortable 90° bend of the arm on top of the subject's thigh. Figure 23 shows a summary of each step taken during the static test protocol. For the first beep, the subject was to move their arm from the rest position towards the device in a ready-to-grip position. For the second beep, the subject was instructed to start pulling the device upwards without stopping until they heard the third beep. After hearing the third beep, subjects were instructed to release the device and return to the rest position to conclude the end of the

static test. The static test was repeated a total of five times. Subjects were asked if they needed a break before continuing on to the dynamic tests.

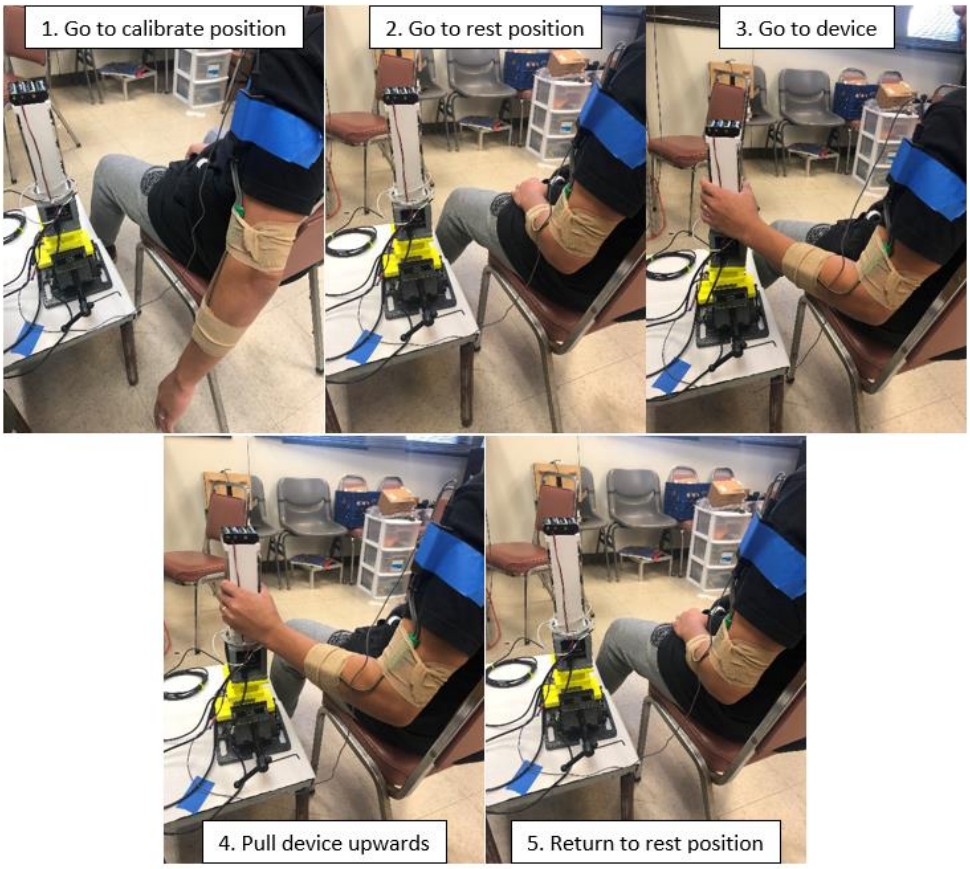

FIGURE 23. Static test protocol.

For the dynamic test scenarios, the device was removed from vise's adapter unit. The device was placed on top of the adapter unit to keep the device at the same level as it was for the static testing. The first dynamic test case was performed without additional weights added to the device. Once again, subjects were asked to extend their arms to calibrate the sensors, and return to rest position at the end of calibration. Subjects were reminded on the actions they were to perform for dynamic testing. For the first beep, from the resting position, subjects were instructed lift the device. For the second beep, subjects were instructed to hold the device in place. For the third beep, subjects were instructed to place the device back on top of the vise's

adapter unit. The third beep concluded the end of the first dynamic test. The dynamic test case without weights was repeated five times. After, the weight compartment was attached to the device with a load of 515 grams and the dynamic test was repeated an additional five times. The protocol for dynamic testing is summarized in Figure 24 below. Subjects were asked if they needed a break before switching arms and repeating the experiment.

FIGURE 24. Dynamic test protocol.

After dynamic testing of the right hand, the experiment was repeated on the left hand. The subject's chair was also rotated 180° and the subject was asked to adjust themselves comfortably again. Then the goniometer was removed from the subject's right arm and attached to their left arm. As previous, the subject was allowed to take breaks in between tests if desired.

5.3 Baseline Data Collection

As discussed in earlier sections, a LabVIEW virtual instrument was used to monitor and collect subject data that was fed by an Arduino. After each session, the virtual instrument saved the data under a unique and descriptive file name for further evaluation. Post processing scripts were developed in MATLAB to help provide the variables necessary for grip force, load force, and elbow angle assessment. Figure 25 shows the different stages of the data collection process for this study.

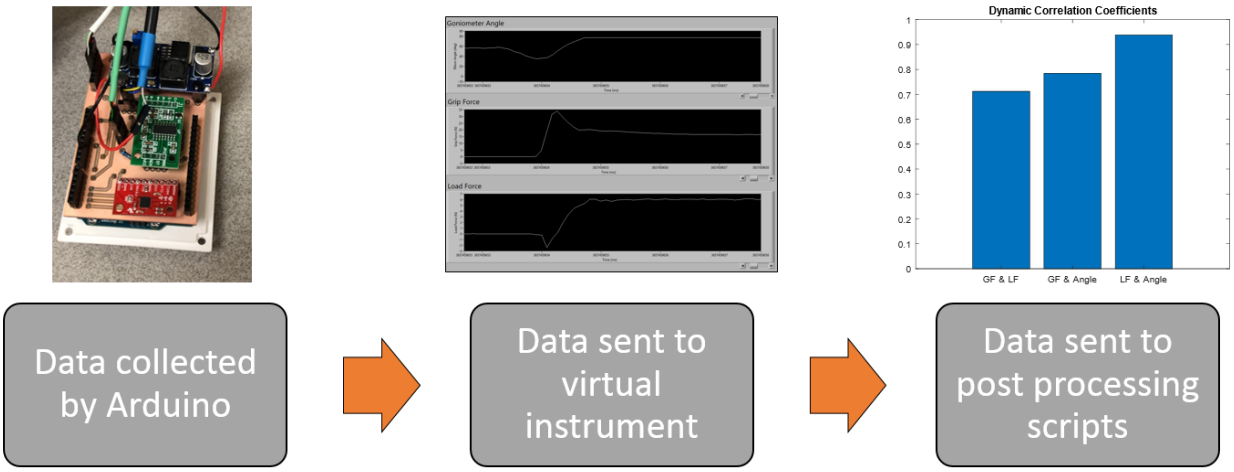

FIGURE 25. Data collection overview.

The post-processing MATLAB scripts generated an Excel sheet for each test case with the assessment variables for each of the five trials. With a total of 16 individual tests per hand per subject per round (1 max grip, 5 static and 5 dynamic without added weights, 5 dynamic with weights), in the end, there was a total of 320 data sets that served as baseline data for all five subjects for both hands for each test scenario. The assessment variables were G/L (grip-to-load) ratio, the correlation coefficients, the time delays, and the gains and offsets from linear regression scatter plots for grip force, load force, and elbow angle. The average lifting and

lowering arm speed for the dynamic task were also computed using the elbow angle and the time between the beeps of 3.5s. The next chapter will discuss the different phases that were evaluated per test case and provide insight on subject data and analysis on system reliability.

CHAPTER 6

RESULTS AND DATA ANALYSIS

The baseline data collected was post processed in MATLAB and coordination assessment variables were calculated. The post processing scripts split the data into different phases for evaluation and were dependent of the type of test conducted. Grip-to-load ratio, correlation coefficients, coupling, and modulation were calculated during each phase for grip force, load force, and elbow angle. Elbow speeds during lifting and lowering were also calculated, along with the lifting-to-lowering speed ratio, but only for dynamic testing. Table 1 provides the list all of the variables that will be referred to in this chapter, along with their abbreviations, where the subscript GL describes the relationship between grip force (G) to load force (L), subscript GE describes the relationship between grip force (G) to elbow angle (E), and subscript LE describes the relationship between load force (L) to elbow angle (E).

The list of equations below are used to calculate the grip-to-load ratio, correlation coefficients, coupling variables (correlation coefficients and time lags), modulation variables (gains and offsets), and lifting-to-lowering speed ratios. The grip-to-load ratio was calculated as,

$$G/L = \frac{G_{avg}}{L_{avg}}, \tag{9}$$

where G/L is a unitless grip-to-load, G_{avg} is the average of the grip load and L_{avg} is the average of the load force in N. The correlation coefficients and time lags were obtained by using MATLAB's corr2(x,y) built-in function, where x and y and the vectors to be compared. The modulation variables, gains and offsets, were retrieved from the grip force versus load force, grip force versus elbow angle, and load force versus elbow angle scatter plots. By using MATLAB's scatter(x,y) function and obtaining the linear equation for grip force, load force, and elbow angle,

the gains were retrieved from the linear slopes and offsets were obtained from the linear b-intercepts. In MATLAB's built-in scatter function, x and y are the two vectors being plotted. The lifting and lowering speeds were calculated by using Equation (10) and (11)

$$\dot{\theta}_{e,lift} = \frac{E_{lift,end} - E_{lift,start}}{t_{lift,end} - t_{lift,start}}, \tag{10}$$

$$\dot{\theta}_{e,lower} = \frac{E_{lower,end} - E_{lower,start}}{t_{lower,end} - t_{lower,start}}, \tag{11}$$

where $\dot{\theta}_{e,lift}$ and $\dot{\theta}_{e,lower}$ are the elbow lifting and lowering speeds in degrees/second, $E_{lift,end}$ and $E_{lift,start}$ are the elbow angles at the end and start of lifting in degrees, $t_{lift,end}$ and $t_{lift,start}$ are the times at the end and start of lifting in seconds, $E_{lower,end}$ and $E_{lower,start}$ are the elbow angles at the end and start of lowering in degrees, and $t_{lower,end}$ and $t_{lower,start}$ are the times at the end and start of lowering in seconds.

For static testing, the data were analyzed in two different phases. After the second beep, a subject is prompted to start pulling the device upwards. The pulling portion of the test is Phase 1 in static testing and illustrated in Figure 26. Phase 2 occurs after the third beep, when a subjected is instructed to release the device.

For dynamic testing, the data was split into three different phases. Phase 1 occurs after the first beep and was designated to capture hand forces and elbow movements when a subject lifted the device. Phase 2 occurs right after the second beep and was used to detect any arm and hand instability when holding the device in mid-air for a few seconds. The third beep, initiated Phase 3 which was used to capture hand and elbow movement patterns when lowering the device back down. The phases for dynamic testing are illustrated in Figure 27 below. This chapter will provide an overview of the raw data collected during each experiment session, the assessment

variables that were used to provide coordination analysis, a comparison between the findings of this study and those from literature, and will end with an analysis in device reliability.

TABLE 1. Static and Dynamic Variable Names

Variable	Static Variable Names	Dynamic Variable Names	Equation
G/L	Grip-to-load ratio	Grip-to-load ratio	Equation (9)
R_{GL}	Correlation Coefficient	Correlation Coefficient	MATLAB corr2(G,L)
R_{GE}			MATLAB corr2(G,E)
R_{LE}			MATLAB corr2(L,E)
$td_{1,\,GL}$	Time delay for phase 1 (Pull)	Time delay for phase 1 (Lift)	MATLAB corr2(G,L)
$td_{1,\,GE}$			MATLAB corr2(G,E)
$td_{1,\,LE}$			MATLAB corr2(L,E)
$td_{2,\,GL}$	Time delay for phase 2 (Release)	Time delay for phase 2 (Hold)	MATLAB corr2(G,L)
$td_{2,\,GE}$			MATLAB corr2(G,E)
$td_{2,\,LE}$			MATLAB corr2(L,E)
$td_{3,\,GL}$	-	Time delay for phase 3 (Lower)	MATLAB corr2(G,L)
$td_{3,\,GE}$			MATLAB corr2(G,E)
$td_{3,\,LE}$			MATLAB corr2(L,E)
m_{GL}	Gain	Gain	MATLAB scatter (G,L)
m_{GE}			MATLAB scatter (G,L)
m_{LE}			MATLAB scatter (G,L)
b_{GL}	Offset	Offset	MATLAB scatter (G,L)
b_{GE}			MATLAB scatter (G,L)
b_{LE}			MATLAB scatter (G,L)
$\dot{\theta}_{lift}$	-	Lifting elbow speed	Equation (10)
$\dot{\theta}_{lower}$		Lowering elbow speed	Equation (11)

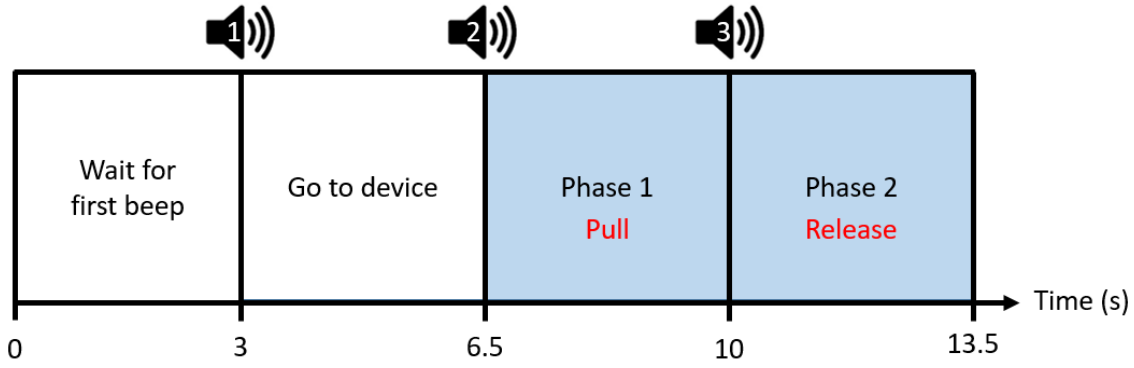

FIGURE 26. Static test phases.

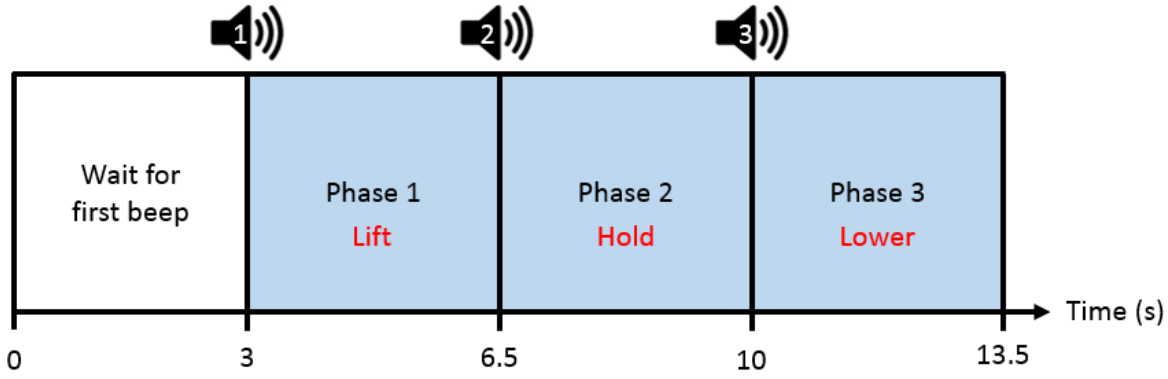

FIGURE 27. Dynamic test phases.

6.1 Data Processing

This subsection explores the data patterns and processing approaches for grip force, load force, and elbow angle for all test cases using sample data collected from one of the subjects (subject 3). Note that the experiment was repeated twice, with a week in between to validate the system reliability. The sample subject data was selected from a trial in the first test session. The overall data analysis across all five subjects will be presented in the next subsections.

Session one began with a measurement of each subject's maximum grip force. As previously described, this test prompts the subject to grip the device as hard as they could at the

start of each beep. Subjects were instructed to grip and hold the device a total of three times following each beep. The subject was recommended to grip for less than one second to avoid fatigue for the following static and dynamic tests. Figure 28 displays the maximum grip force values collected for the left and right hand for subject three. The left-hand maximum grip force was averaged to be 77.37 N, while their right-hand maximum grip force was averaged to be 85.51 N. The maximum grip values for all subjects will be discussed in detail in the following section. The values will also be compared to what has been found in literature.

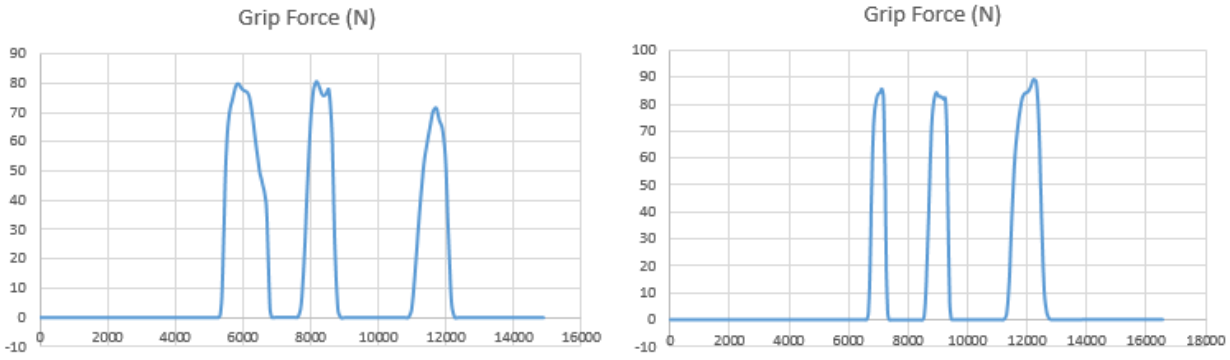

FIGURE 28. Sample data of maximum grip forces for subject three (left: left hand, right: right hand).

Next is the static tests for the left and right hand. The experimental procedure for this test is described in the previous chapter. Figure 29 displays the elbow angle, grip force, and load force for each hand and has vertical dashed lines that indicate the start and the end of each of the static phases. The sets of plots below display the hand and arm movements during static testing of the subject. For both hands, elbow angle was not detected beyond 100°, since all subjects naturally maintained their elbow angle close to 90° throughout testing. Grip force levels ranged from 0-50 N and grip force levels ranged 0-20 N.

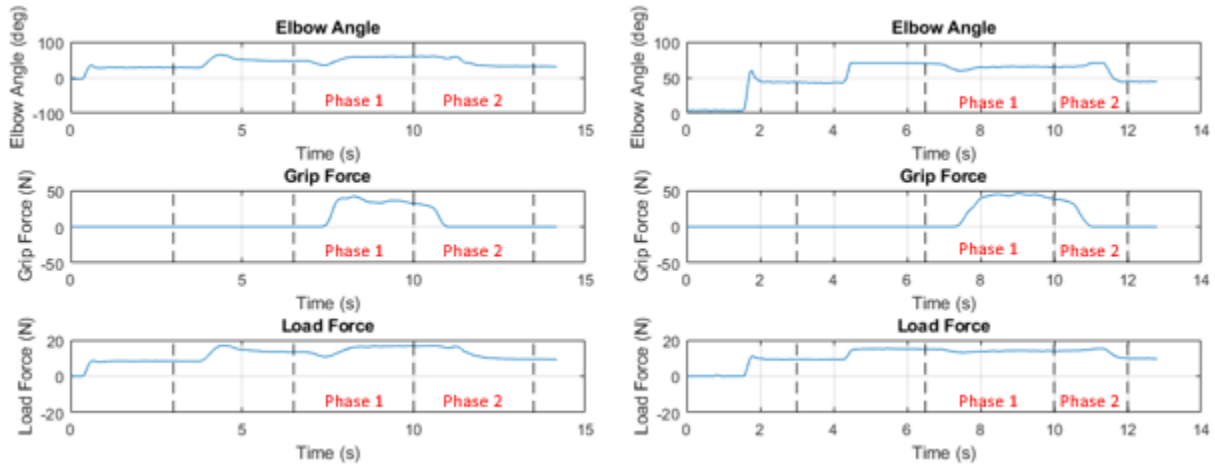

FIGURE 29. Raw data for static tests for subject three (left: left hand, right: right hand), where phase 1 indicates pulling and phase 2 indicates releasing.

The next set of tests were the dynamic tests. To start dynamic testing, the subject was tested without weights and followed with a second test with weights for each hand. Figure 30 displays the elbow angle, grip force and load force for the dynamic test case without weights and Figure 31 displays the data for the dynamic test case with weights added to the device. As mentioned in the previous paragraph, the vertical dashed lines in the plots in indicate the start and end of each of the dynamic phases. The plots below show high similarities between dynamic testing with weights and without weight. The elbow angle does not extend beyond 100° for both hands, just like in the static tests. Also, the force ranges vary slight but stay within the same ranges of 0-10 N for grip force and 0-5 N for the load force. The grip force range is much more comparable to what is in literature for the dynamic tests when compare to the static tests. The following section will provide a more detailed assessment of the coordination between grip force to load force, grip force to elbow angle, and load force to elbow angle.

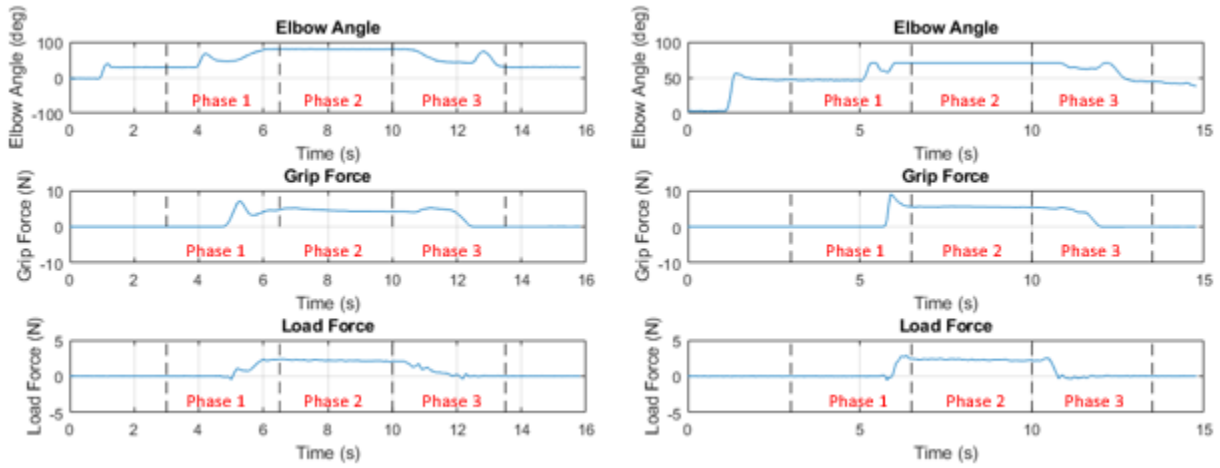

FIGURE 30. Raw data for dynamic tests without weights for subject three (left: left hand, right: right hand), where phase 1 indicates lifting, phase 2 indicates holding and phase 3 indicates lowering.

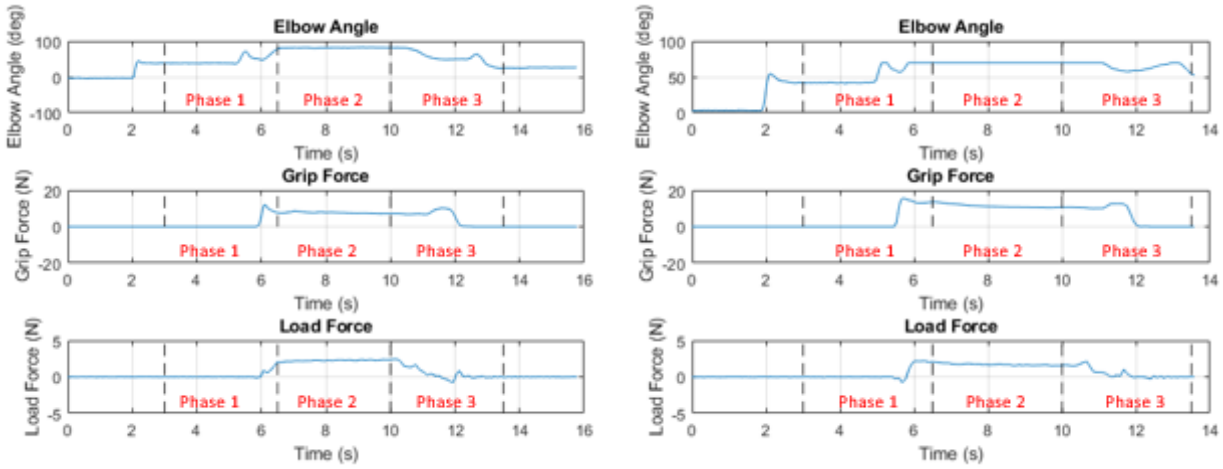

FIGURE 31. Raw data for dynamic tests with weights for subject three (left: left hand, right: right hand), where phase 1 indicates lifting, phase 2 indicates holding and phase 3 indicates lowering.

6.2 System Reliability Validation

To measure system reliability, an intraclass coefficient (ICC) analysis was performed on the data that was collected between the first and the second test sessions. Three variables are used in the reliability validation of the device: grip force, load force, elbow angle, lifting speed, and lowering speed. An intraclass coefficient was computed in MATLAB. The ICC coefficient

of 1 indicates the highest reliability between the groups, which indicates that the system is reliable. The ICC analysis was conducted for each test case using all of the subject trials collected for each session.

The first variable that was evaluated for system reliability was grip force. The average grip force was taken for each subject trial, and a comparison was made between sessions. The ICC values for grip force are displayed in Table 2. As shown in the table below, the ICC values for grip force range from 0.501 to 0.895. Overall, based on the analysis, the ICC values show that the system is somewhat reliable to high reliable when observing grip force. The system proved to be the most reliable during the left-hand dynamic tests with the use of weights and the least reliable during left-hand static tests. This analysis also shows that the left hand has higher ICC values for grip force than the left hand during the dynamic tests, with or without the use of weights. During the static tests, the left hand shows to be lower in ICC value than the right hand. The ICC values for grip force show support some reliability level to the device when collecting this grip force measurements.

TABLE 2. Intraclass Coefficient Values for Grip Force for All Subjects During Each Test Session.

Test Case	ICC
Dynamic test (left hand, no weight)	0.646
Dynamic test (left hand, with weight)	0.895
Dynamic test (right hand, no weight)	0.504
Dynamic test (right hand, with weight)	0.702
Static test (left hand)	0.501
Static test (right hand)	0.763

The second variable that was evaluated for system reliability was load force. The average load force was taken for each subject trial, and a comparison was made between sessions. The

ICC values for load force are displayed in Table 3. As shown in the table below, the ICC values for load force are significantly lower than those for grip force. The ICC values range from -0.1423 to -0.1076. Since the ICC values for load force are low and mostly negative, they do not support system reliability when collecting load force measurements. Subjects were asked to lift the hand function assessment device naturally as they would a cup of water. The low values can be due to how each subject lifting the object, since load force is derived from acceleration. Each subject also lifted the device at different speeds and is explore in the upcoming paragraphs during the ICC analysis for lifting an lowering speeds.

TABLE 3. Intraclass Coefficient Values for Load Force for All Subjects During Each Test Session.

Test Case	ICC
Dynamic test (left hand, no weight)	-0.1423
Dynamic test (left hand, with weight)	-0.1102
Dynamic test (right hand, no weight)	-0.1092
Dynamic test (right hand, with weight)	-0.1076

The third variable that was evaluated for system reliability was elbow displacement. The elbow displacement was taken for each subject trial, and a comparison was made between sessions. The elbow displacement was taken as the elbow angle difference between the last and the first elbow angle measurement. The ICC values for elbow displacement are displayed in Table 4. As shown in the table below, the ICC values for elbow displacement are lower than those for grip force, but higher in value that those for load force. The ICC values range from -0.0264 to 0.5498. The systems to have the highest ICC value during left hand dynamic testing without the use of weights. However, an ICC value of 0.5498 is significantly lower than 1 and does not support high reliability. Since the ICC values for elbow displacement are on the low end, they do not support system reliability when collecting elbow displacement measurements.

TABLE 4. Intraclass Coefficient Values for Elbow Displacement for All Subjects During Each Test Session.

Test Case	ICC
Dynamic test (left hand, no weight)	0.5498
Dynamic test (left hand, with weight)	-0.0264
Dynamic test (right hand, no weight)	0.5039
Dynamic test (right hand, with weight)	0.397

The fourth variable that was evaluated for system reliability was elbow lifting speed. The elbow lifting speed was taken for each subject trial, and a comparison was made between sessions. The elbow lifting speed was taken as the difference between angle difference/time difference during lifting. Elbow lifting speed was only measured during dynamic testing, since the elbow angle was mainly stationary during static testing. The ICC values for elbow displacement are displayed in Table 5. The ICC values range from -0.2069 to 0.2737. Similar to the ICC values for elbow displacement, the ICC values for elbow lifting speed also have wide variability since the values resulted are both negative and positive. Even the largest ICC value resulted from left hand dynamic testing with the use of weights, is on the low end for system reliability. Since the ICC values for elbow lifting speed are on the low, they do not support system reliability when collecting elbow lifting speed measurements.

TABLE 5. Intraclass Coefficient Values for Elbow Lifting Speed for All Subjects During Each Test Session.

Test Case	ICC
Dynamic test (left hand, no weight)	-0.2069
Dynamic test (left hand, with weight)	0.2737
Dynamic test (right hand, no weight)	-0.1109
Dynamic test (right hand, with weight)	0.0386

The last variable that was evaluated for system reliability was elbow lowering speed. The elbow lowering speed was taken for each subject trial, and a comparison was made between

sessions. The elbow lowering speed was taken as the difference between angle difference/time difference during lowering. Just like for lifting speed, lowering speed was only measured during dynamic testing for the same reason that the elbow angle was kept stationary during static tests. The ICC values for elbow displacement are displayed in Table 6. The ICC values range from 0.1218 to 07279. The largest ICC value resulted from right hand dynamic testing with the use of weights, while the smallest ICC value resulted from left hand dynamic testing without the use of weights. The ICC values for lowering speed are all positive in value, but vary significantly between each test case. Since the ICC values for elbow lower speed are vary so much, they do not support system reliability when collecting elbow lowering speed measurements.

TABLE 6. Intraclass Coefficient Values for Elbow Lowering Speed for All Subjects During Each Test Session.

Test Case	ICC
Dynamic test (left hand, no weight)	0.1218
Dynamic test (left hand, with weight)	0.395
Dynamic test (right hand, no weight)	0.3719
Dynamic test (right hand, with weight)	0.7279

To collectively summarize the ICC results, every variable used for ICC analysis did not result in system reliability. Possible reasons to why the system could not provide repeatable measurements may be due to various reasons. One possible cause to why the system resulted to be unreliable may be due to subject placement relative to the hand function assessment device. The device was placed on a table on top of a vise for all test cases, but the height was not adjusted for each subject and the distance between a subject's arm and the device was not measured and therefore not kept consistent. Another possible cause may be due to the sensor selection for sensors. The load cells that were used for this work could detect up to 50 pounds of mass. Perhaps different loads cells that are meant to measure smaller loads could result data that

is more accurate, since the load cells would be more sensitive to smaller loads. The goniometer used also varied in readings, and a sensor more suited for elbow measurements should be considered for future experiments.

6.3 Coordination Assessment

A hand force coordination assessment was conducted across all five subjects to obtain baseline data. In literature, the grip-to-load ratio, force coupling and grip force modulation were used to assess force coordination. For this study, arm movement measurements were included to help gain insight on the coordination between hand forces and arm movement. The results from the maximum grip force test are first presented, followed by an assessment of coupling and modulation for hand forces and arm movement measurements.

6.3.1 Maximum Grip Force

In previous literature, the maximum grip force has been reported to range between 3 to 10 Newtons for healthy subjects. For this work, the maximum grip force was collected and averaged for each subject during both testing session. The results obtained for maximum grip force are displayed in Figure 32, along with their standard deviations displayed in Table 7. Based on the results for this work, the maximum grip force ranged from 57.89 to 104.24 Newtons for the left hand and 45.23 to 143.56 N for the right hand. The values for grip force are significantly larger than those found in literature and their values affected the results found during hand force and arm movement coupling and modulation analysis. A possible reason to why the values for grip force resulted large in value can be due to the internal calibration from the LabVIEW virtual instrument. Another reason could for large grip force values could be due to the Omega Load Cell not being calibrated for this work. The sensor was previously calibrated for the old hand

function assessment device, but was not calibrated for the modified hand function assessment device.

TABLE 7. Averaged Maximum Grip Force in Newton with Their Standard Deviation.

Subject	$\bar{x}_{MaxG,left} \pm SD$ (N)	$\bar{x}_{MaxG,right} \pm SD$ (N)
1	57.89 ± 30.26	67.50 ± 12.32
2	65.31 ± 21.36	45.23 ± 24.22
3	78.06 ± 9.03	85.82 ± 4.02
4	104.24 ± 7.87	143.56 ± 4.73
5	98.55 ± 3.85	109.76 ± 18.17

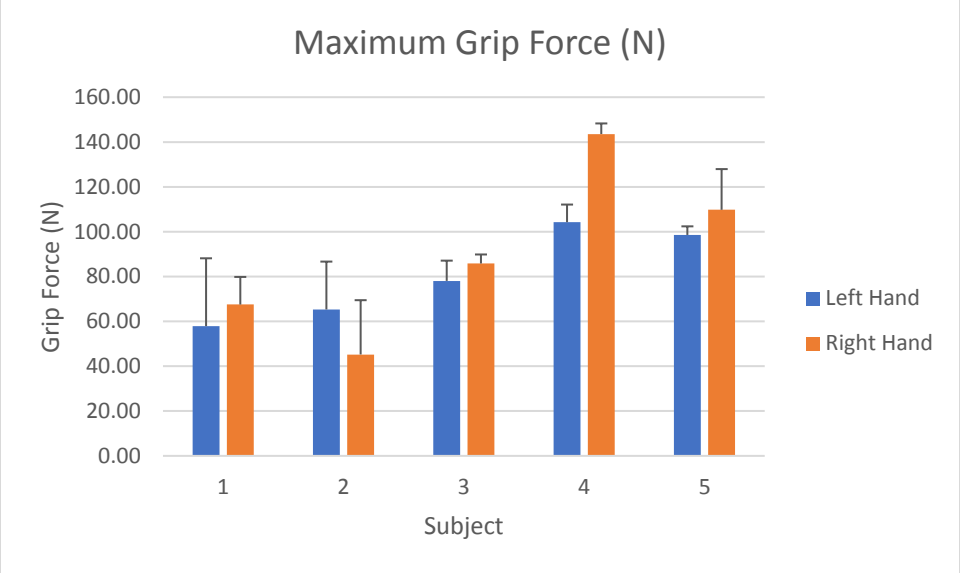

FIGURE 32. Averaged maximum grip force all subjects and all trials.

6.3.2 Hand Force and Arm Movement Coupling

In literature, high coupling of grip force and load force is indicated by a high correlation coefficient and low time lags. Literature has shown that the correlation coefficients for grip force and load force range from 0.8 to 1.0 for healthy individuals and low lag times that range between 0 to 0.04 seconds [2]. Static and dynamic tests were evaluated separately to determine what role arm movement played in hand force coordination. The correlation coefficients and time lags

were calculated for each subject and then the average was taken for every trial for all the subjects. The correlation coefficients and time lags were calculated using MATLAB's corr2 built-in function.

During static testing, the averaged correlation coefficients and averaged time lags were calculated for the pulling (phase 1) and releasing (phase 2) phases for grip force and load force. Elbow angle was not included in this analysis since it was mainly kept at a constant angle. The correlation coefficients can be seen in Figure 33, along with their standard deviations in Table 8. As it can be seen in Figure 33, the correlation coefficient was 0.76 for the left hand and 0.77 for the right hand during static testing. The correlation coefficient for the grip force and load force is slightly below what has been found in literature for healthy young adults.

TABLE 8. Averaged Correlation Coefficient with Their Standard Deviation for Static Testing.

Variable	$\bar{x}_{R,left} \pm SD$	$\bar{x}_{R,right} \pm SD$
R_{GL}	0.76 ± 0.35	0.77 ± 0.34

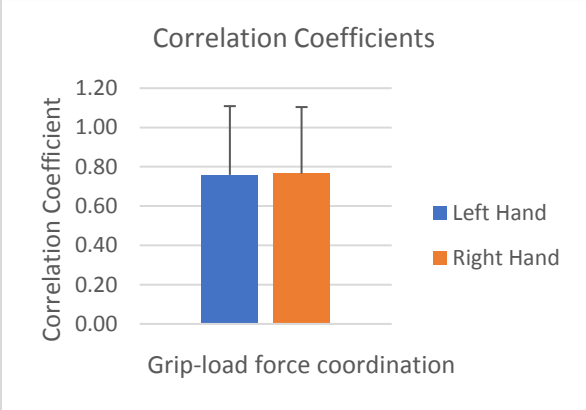

FIGURE 33. Averaged correlation coefficients for all subjects and all trials during static testing.

The time delays for phase 1 and phase 2 and displayed in Figure 34, along with their standard deviations displayed in Table 9. The time lags for the left hand are 0.15 and 0.14

seconds for phase 1 and phase 2, respectively. While, the time lags for the right hand are 0.08 and 0.11 seconds for phase 1 and phase 2, respectively. The time lag corresponding to the right-hand during phase 1 appears to be the one closest to what has been found in literature. Although, every time lag collected for static testing is larger than literature time lag range, the time lags found for this study are not significantly larger. Based on the static coupling analysis for static testing, the data suggests that grip force and load force are high coordinated due to their high correlation coefficients and low time lags.

TABLE 9. Averaged Time Lags in Seconds with Their Standard Deviation for Static Testing for Pulling (Phase 1) and Releasing (Phase 2).

Variable	$\bar{x}_{td,left} \pm SD$ (s)	$\bar{x}_{td,right} \pm SD$ (s)
$td_{1,\,GL}$	0.15 ± 0.25	0.08 ± 0.15
$td_{2,\,GL}$	0.14 ± 0.28	0.11 ± 0.21

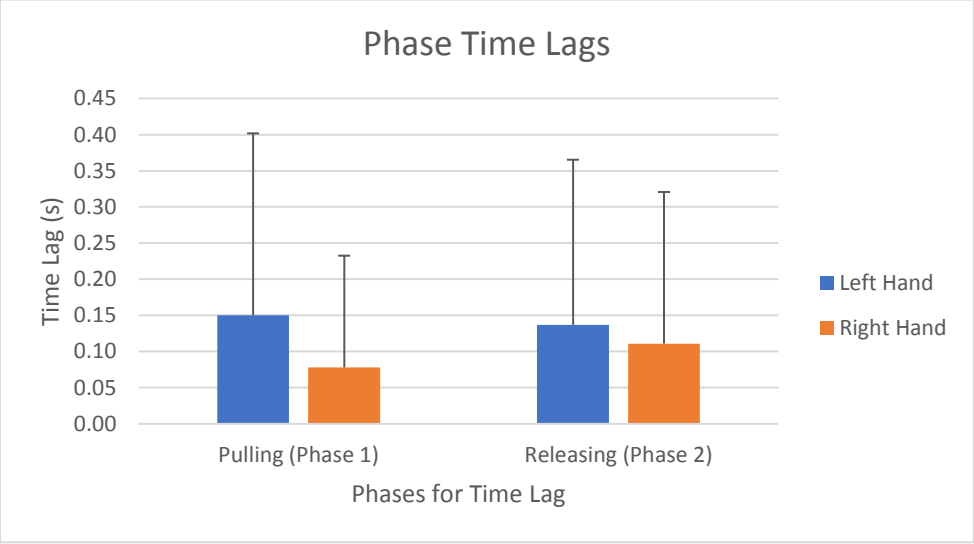

FIGURE 34. Averaged time lags for all subjects and all trials during static testing for pulling (phase 1) and releasing (phase 2).

For dynamic testing, the averaged correlation coefficients and average time lags were calculated for both hands with and without additional weights. The correlation coefficients are displayed in Figure 35 for dynamic tests without the use of weights and with weights, along with

their standard deviations displayed in Table 10. In the figure below, again, the grip-load pair has the highest correlation coefficient value ranging in 0.81 to 0.82 for both weight cases and falls within the literature values. The correlation coefficients for grip-elbow angle and load-elbow angle appear to be lower in value which can mean lower coordination. Also, the left hand during all dynamic tests, has higher correlation coefficients than the right hand for the grip-elbow angle and load-elbow angle pairs.

TABLE 10. Averaged Correlation Coefficients with Their Standard Deviation for Dynamic Tests.

	Without Weights		With Weights	
Variable	$\bar{x}_{R,left} \pm SD$	$\bar{x}_{R,right} \pm SD$	$\bar{x}_{R,left} \pm SD$	$\bar{x}_{R,right} \pm SD$
R_{GL}	0.82 ± 0.05	0.81 ± 0.05	0.85 ± 0.06	0.85 ± 0.06
R_{GE}	0.62 ± 0.08	0.51 ± 0.20	0.69 ± 0.07	0.55 ± 0.18
R_{LE}	0.64 ± 0.15	0.55 ± 0.18	0.66 ± 0.16	0.55 ± 0.15

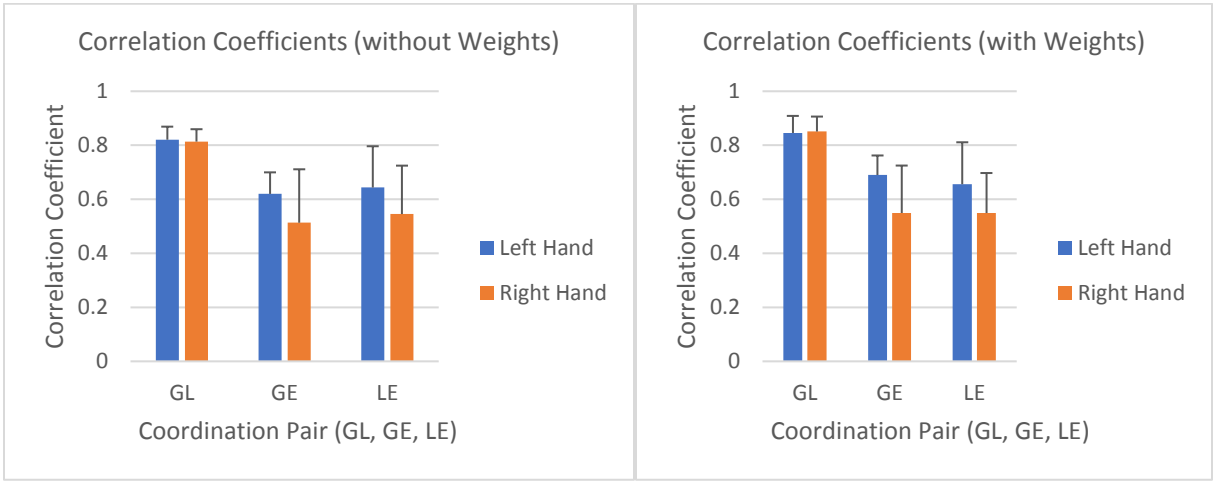

FIGURE 35. Averaged correlation coefficients for all subjects and all trials during dynamic testing without weights.

The time lags for the lifting (phase 1) are displayed in Figure 36 for all dynamic tests, along with their standard deviations in Table 11. For the lifting phase, the data shows low time lags for all of the coordination pairs, but the values are higher than those provided by literature

by about an order in magnitude. The left-hand dynamic test with weights, has the lowest time lag of 0.09 seconds for the grip-load force pair, however, that time lag is still larger than what is in literature. The longest time lag was observed during right hand dynamic testing without weights for the load-elbow angle pair, which results in the lowest coordination during the lift phase.

TABLE 11. Averaged Lifting (Phase 1) Time Lags in Seconds with Their Associated Standard Deviation for Dynamic Tests.

	Without Weights		With Weights	
Variable	$\bar{x}_{td1,left} \pm SD$ (s)	$\bar{x}_{td1,right} \pm SD$ (s)	$\bar{x}_{td1,left} \pm SD$ (s)	$\bar{x}_{td1,right} \pm SD$ (s)
$td_{1,\,GL}$	0.19 ± 0.29	0.15 ± 0.05	0.09 ± 0.23	0.30 ± 0.61
$td_{1,\,GE}$	0.36 ± 0.38	0.36 ± 0.59	0.18 ± 0.28	0.35 ± 0.52
$td_{1,\,LE}$	0.21 ± 0.35	0.52 ± 0.69	0.21 ± 0.32	0.33 ± 0.41

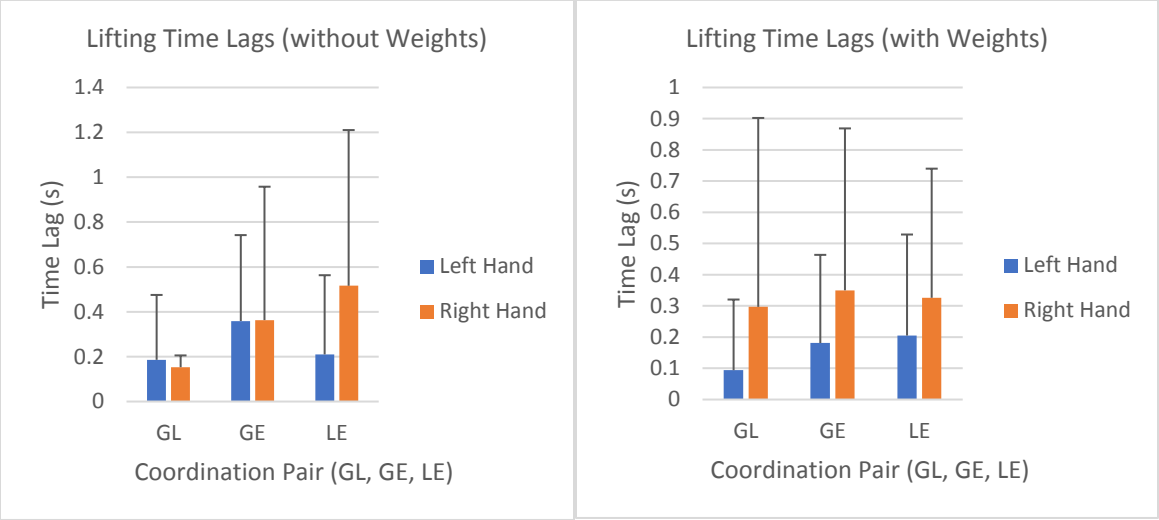

FIGURE 36. Averaged lifting (phase 1) time lags for all subjects and all trials during dynamic testing.

For the holding phase, the time lags in Figure 37 for dynamic testing without the use of weights and with the use of weights, along with their standard deviations displayed in Table 12. The longest time lag found during the holding phase was during right hand dynamic testing without weights and had a value of 0.06 seconds. This value is only 0.02 seconds larger than the

range found in literature. The results suggest that the grip-load, grip-elbow angle, and load-elbow angle pairs all have low time lags that fall within the range found in literature.

TABLE 12. Averaged Holding (Phase 2) Time Lags in Seconds with Their Associated Standard Deviation for Dynamic Tests.

	Without Weights		With Weights	
Variable	$\bar{x}_{td2,left} \pm SD$ (s)	$\bar{x}_{td2,right} \pm SD$ (s)	$\bar{x}_{td2,left} \pm SD$ (s)	$\bar{x}_{td2,right} \pm SD$ (s)
$td_{2,\,GL}$	0.01 ± 0.01	0.04 ± 0.11	0.00 ± 0.00	0.01 ± 0.04
$td_{2,\,GE}$	0.01 ± 0.04	0.04 ± 0.11	0.00 ± 0.00	0.00 ± 0.00
$td_{2,\,LE}$	0.00 ± 0.00	0.06 ± 0.18	0.00 ± 0.00	0.00 ± 0.00

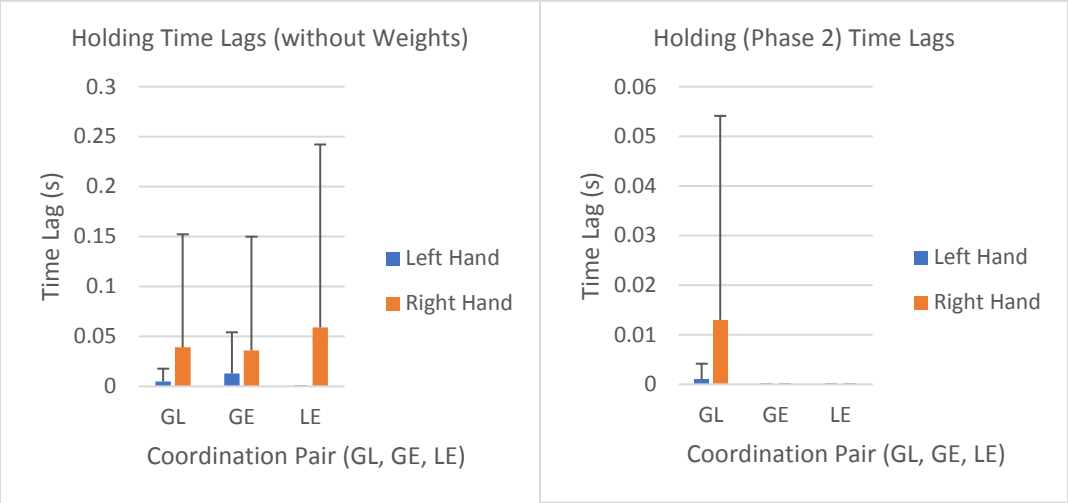

FIGURE 37. Averaged holding (phase 2) time lags for all subjects and all trials during dynamic testing.

For the lowering phase, the time lags in Figure 38 for dynamic testing without the use of weights and with the use of weights, along with their standard deviations displayed in Table 13. The grip-elbow angle pair appears to have the shortest time lag for all dynamic testing, while the grip-load force pair has the longest time lags based from Table 13. In general, the right hand during all dynamic tests and for all coordination pairs also appears to have the higher time lag

values when compared to the left hands. Based on the time lag values for during the lowering phase, it appears that the grip-elbow angle has the highest coordination, with the load-elbow angle pair also showing high coordination. The grip-load force pair displays the lowest coordination, according to Table 13.

TABLE 13. Averaged Lowering (Phase 3) Time Lags in Seconds with Their Associated Standard Deviation for Dynamic Tests.

	Without Weights		With Weights	
Variable	$\bar{x}_{td3,left} \pm SD$ (s)	$\bar{x}_{td3,right} \pm SD$ (s)	$\bar{x}_{td3,left} \pm SD$ (s)	$\bar{x}_{td3,right} \pm SD$ (s)
$td_{3,\,GL}$	0.12 ± 0.12	0.21 ± 0.13	0.11 ± 0.13	0.13 ± 0.17
$td_{3,\,GE}$	0.00 ± 0.00	0.01 ± 0.02	0.00 ± 0.00	0.00 ± 0.00
$td_{3,\,LE}$	0.05 ± 0.10	0.06 ± 0.06	0.04 ± 0.07	0.09 ± 0.11

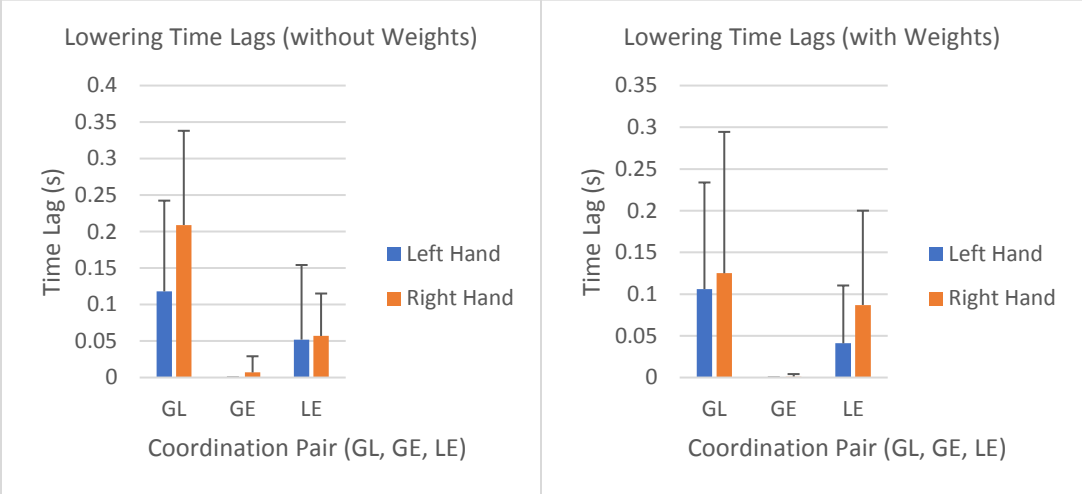

FIGURE 38. Averaged lowering (phase 3) time lags for all subjects and all trials during dynamic testing.

6.3.3 Hand Force and Arm Movement Modulation

High grip force modulation in literature is indicated by high gains and low offsets from regression line equations in the grip force and load force plots. In literature, high modulation has

been observed with gains ranging from 0.5 to 1.0, and offsets ranging from 0 to 2 [2]. A similar analysis was conducted to explore the effects of elbow angle with hand forces.

During static testing, a modulation analysis was conducted to assess the coordination between grip force and load force. The linear gains and offsets for static testing are display in Figure 39, along with their standard deviations displayed in Table 14. Figure 39 shows that the gains values for the right and left hand are very close in value of 0.27 and 0.28, respectively. The gains for both hands are lower than those gains found in literature. The left hand was observed to have an offset value of 3.49 and the right hand had a value of 2.84. The offsets for both hands were higher than those found in literature. Since the gains are relatively similar, and the left hand has a larger offset when compared to the right hand, the left hand appears to have lower coordination of hand forces.

TABLE 14. Averaged Linear Gains and Offsets with Their Associated Standard Deviation for Static Testing.

Variable	$\bar{x}_{left} \pm SD$	$\bar{x}_{right} \pm SD$
m_{GL}	0.27 ± 0.19	0.28 ± 0.18
b_{GL}	3.49 ± 5.82	2.84 ± 4.96

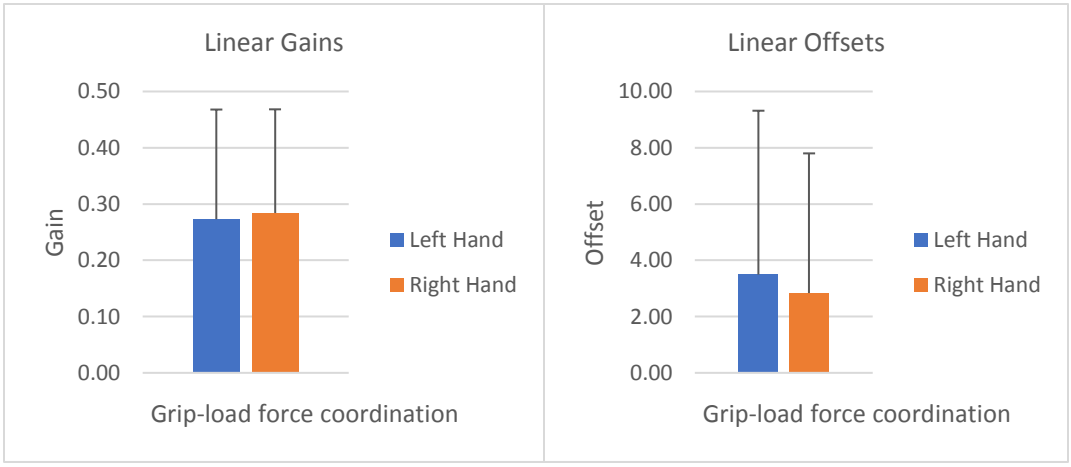

FIGURE 39. Averaged linear gains and offsets for all subjects and all trials during static testing.

During dynamic testing, the gains and offsets were also calculated for grip-load, grip-elbow angle, and load-elbow angle pairs. The gains for the dynamic test results without the use of weights and with weights can be seen on Figure 40, along with their standard deviations displayed in Table 15. As shown in Figure 40, the load-elbow angle gains are higher than the grip-load and grip-elbow angle pairs. The highest gains were found during left-hand dynamic testing with the use of weights. Also, it can be seen from Table 15, that the left hand had larger gains that the right hand during all dynamic testing and for every coordination pair. Only the gains for the grip-load force pair are lower in value that those found in literature, and the grip-elbow angle and load-elbow angle pairs gain values were higher than the literature range for hand forces.

TABLE 15. Averaged Linear Gains with Their Associated Standard Deviation for Dynamic Tests.

	Without Weights		With Weights	
Variable	$\bar{x}_{m,left} \pm SD$	$\bar{x}_{m,right} \pm SD$	$\bar{x}_{m,left} \pm SD$	$\bar{x}_{m,right} \pm SD$
m_{GL}	0.19 ± 0.24	0.47 ± 0.60	0.11 ± 0.12	0.26 ± 0.31
m_{GE}	2.15 ± 1.76	1.69 ± 1.63	1.51 ± 1.41	1.10 ± 1.18
m_{LE}	15.83 ± 7.69	6.28 ± 7.09	16.95 ± 8.82	5.81 ± 5.23

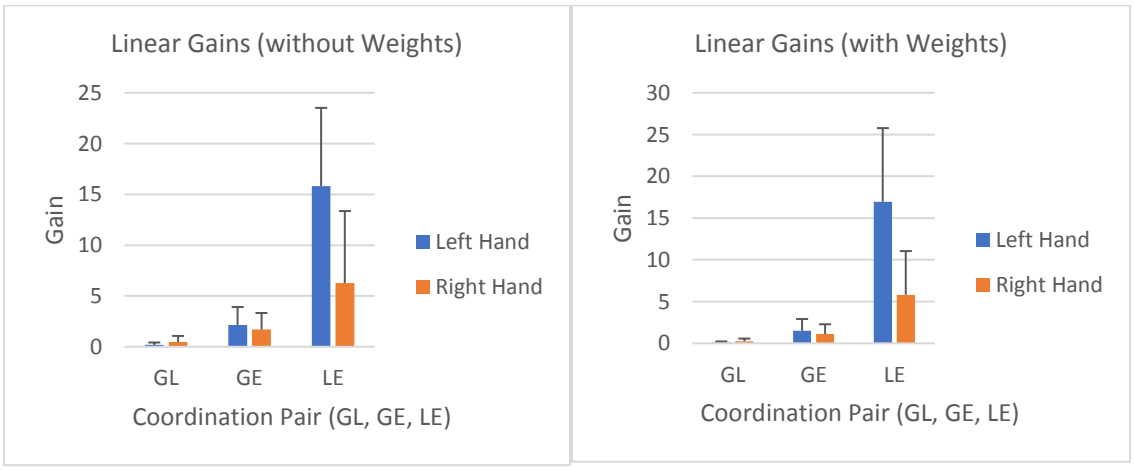

FIGURE 40. Averaged linear gains for all subjects and all trials during dynamic testing.

Figure 41 displays the linear offsets for dynamic testing without the use of weights and with the use of weights weight, along with their standard deviations are displayed in Table 16. The offsets found for the grip-elbow angle and load-elbow angle pairs are significantly larger than those found in literature. The largest offset was found during right hand dynamic testing with the use of weights and had a value of 47.19. The offsets found for the grip-load force pair are lower than those found in literature. The lowest offset was found during right hand dynamic testing with the use of weights as well, and had a value of -0.06. This suggests that the grip-load force pair is more coordination that the other pairs due to their low offset values. The data also suggests that the elbow angle is not highly coordinated with the hand forces.

TABLE 16. Averaged Linear Offsets with Their Associated Standard Deviation for Dynamic Tests.

	Without Weights		With Weights	
Variable	$\bar{x}_{b,left} \pm SD$	$\bar{x}_{b,right} \pm SD$	$\bar{x}_{b,left} \pm SD$	$\bar{x}_{b,right} \pm SD$
b_{GL}	0.09 ± 0.23	0.31 ± 0.92	-0.01 ± 0.05	-0.06 ± 0.10
b_{GE}	42.85 ± 7.52	46.01 ± 9.71	41.84 ± 5.89	45.82 ± 10.57
b_{LE}	43.93 ± 8.66	46.90 ± 9.88	44.46 ± 7.99	47.19 ± 10.61

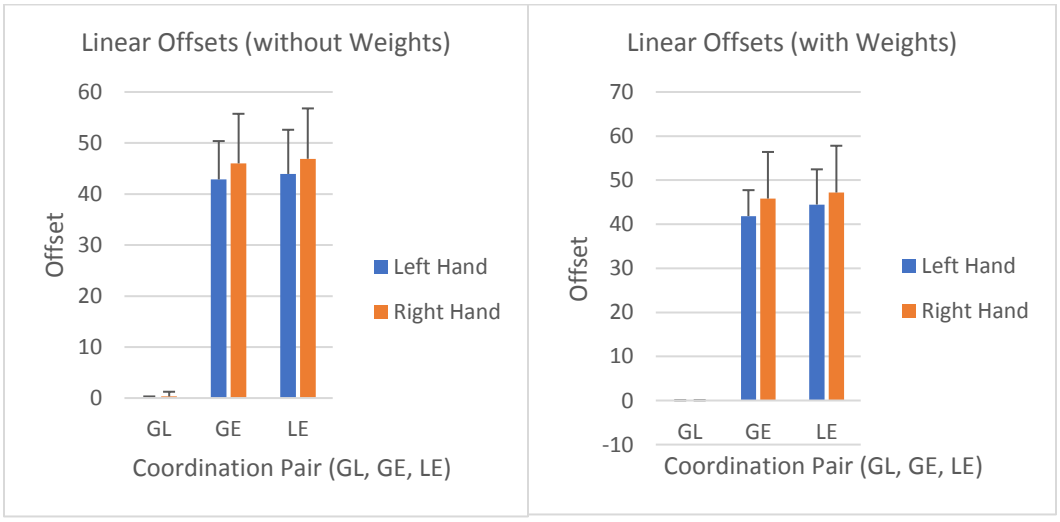

FIGURE 41. Averaged linear offsets for all subjects and all trials during dynamic testing.

Based on the observations collecting during coupling and modulation analysis, it has been collectively concluded that arm movement is not high coordinated with hand forces. Arm movement coordination resulted in low correlation coefficients higher time lags than those found in literature for hand forces. Also, arm movement coordination also resulted in high gains and extremely high offsets, which suggest that elbow angle is not highly coordinated with hand forces.

CHAPTER 7

CONCLUSIONS AND FUTURE WORK

A two degree-of-freedom hand function assessment device, that was previously used to measure grip force and load force only, was modified into a three degree-of-freedom system to also measure elbow angle. This modified device was used to study the coordination between hand forces and arm movements. An experiment was conducted on five healthy young adults to generate baseline data for the device and to provide insight on their hand force and arm movement coordination. An intraclass coefficient analysis and coordination assessment were conducted and resulted in low device reliability and low elbow coordination to grip force and load force. Based on the system reliably test with the intraclass coefficient analysis and the coordination assessment conducted in the previous chapter, the device will need to be further investigation with additional experimentation. Future data sets can help improve the systems repeatability and gain a better understanding of the influence arm movements plays in relation to the hand forces during static and dynamic manipulation tasks. However, the device demonstrates a good starting point for future research studies.

Although the device used for this study is an improvement of the previous device, there are additional modifications that would generate a more optimal and repeatable device. The first recommendation is to modify the electronics chassis to include a compartment for the batteries used to provide power to the Futek load cell. Currently, the batteries are on top of the device which require a need to pass wires from the top of the device to the electronics chassis. This wiring setup occasionally caught subjects off-guard during testing, and caused some patients to slow down to avoid tangling their hands between the wires. Another recommendation is in relation to the mechanical set up. With the current device, it had to be bolted on to a vise to

prevent it from moving during static testing. However, since the vise is not bolted on to the table, subjects would occasionally find themselves lifting the device with the vise off the table ever so slightly. This resulted in the pulling and releasing actions for static testing, not as smooth as they could have been.

Other changes that can be made are to the LabVIEW virtual instrument. Currently, the virtual instrument calibrates the system every single time a session trial is conducted. The architecture of the virtual instrument could be improved so that it only calibrates the system once during the entire session to allow for faster testing. Also, it would be beneficial to collect the raw sensor values in a text file, instead of calculating the grip force, load force, and elbow angle within the virtual instrument source code. The reason for this, is that if there is a mistake in the calculation, a patch must be written in the post processing tools which can be difficult to debug. Having the raw sensor values would also help gain a better understanding of their value and meaning in relation to what is in literature.

A last recommendation for this version of the device is to develop completely automatic post processing scripts. The scripts that were used to process the data for this device were half automatic and half manual, and some data was also processed in excel. This made the post processing of data tedious and long.

APPENDICES

APPENDIX A

EAGLE SCHEMATIC AND BOARD LAYOUT

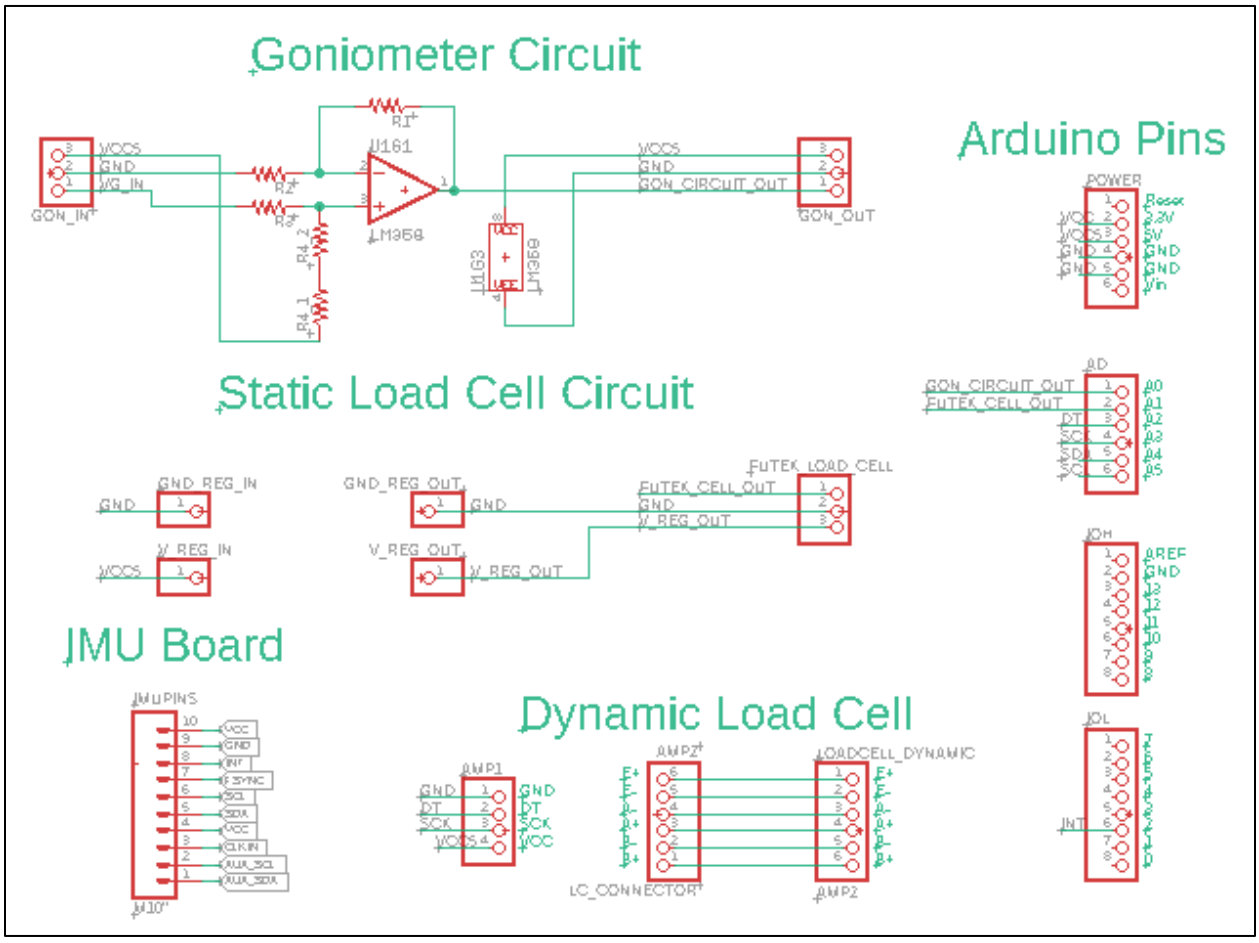

FIGURE 42. Eagle schematic.

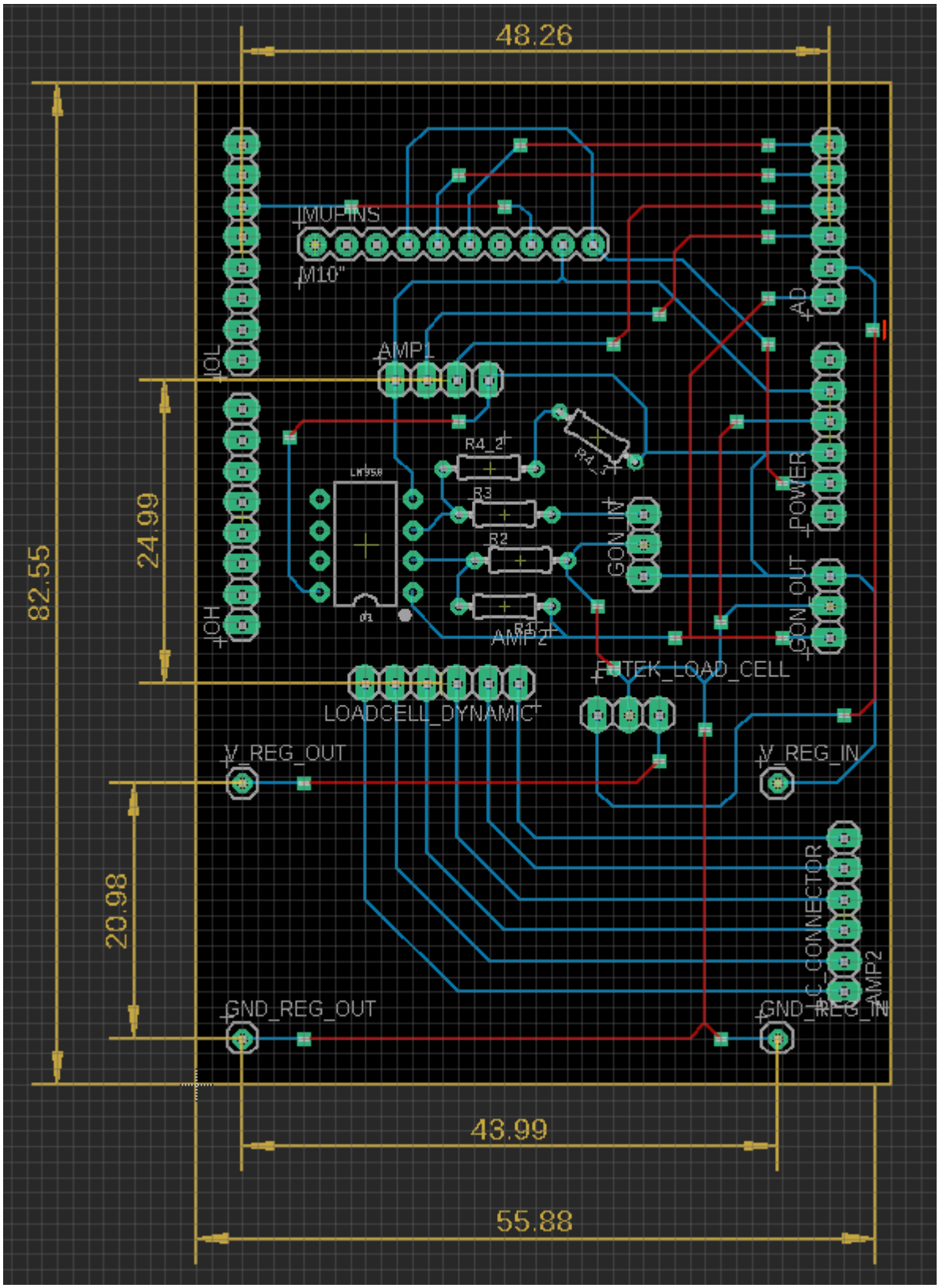

FIGURE 43. Eagle board layout.

APPENDIX B

CALIBRATION DATA

TABLE 17. Goniometer Calibration Data for -120° to -5°

Voltage (mV)	Angle (deg)
0	-120
0	-115
0	-110
0	-105
0	-100
0	-95
0	-90
14	-85
83	-80
151	-75
224	-70
298	-65
366	-60
439	-55
513	-50
591	-45
664	-40
738	-35
816	-30
894	-25
977	-20
1050	-15
1133	-10
1212	-5

TABLE 18. Goniometer Calibration Data for 0° to 120°

Voltage (mV)	Angle (deg)
1295	0
1368	5
1441	10
1515	15
1598	20
1671	25
1749	30
1827	35
1906	40

TABLE 18. Continued.

1984	45
2057	50
2135	55
2214	60
2297	65
2370	70
2443	75
2521	80
2600	85
2678	90
2756	95
2829	100
2913	105
2991	110
3074	115
3152	120

TABLE 19. Futek Load Cell Calibration Data

Output Voltage (V)	Load (lb)
0.855	0.000
1.363	2.205
1.608	3.307
1.862	4.409
2.13	5.677
2.453	7.132
2.888	9.039
3.123	10.064
3.235	10.582
3.558	12.037
3.988	13.944
4.217	14.969
4.54	16.424
4.97	18.331

REFERENCES

[1] Barbosa de Freitas, P., Krishnan, V., and Jaric, S., 2008, "Force Coordination in Object Manipulation," Journal of Human Kinetics, vol. 20(1), pp. 37-50.

[2] Krishnan, V., and Jaric, S., 2008, "Hand Function in Multiple Sclerosis: Force Coordination in Manipulation Tasks," Clinical Neurophysiology, vol. 119(10), pp. 2274–2281.

[3] Krishnan, V., Barbosa de Freitas, P., and Jaric, S., 2008, "Impaired Object Manipulation in Mildly Involved Individuals with Multiple Sclerosis," Motor Control, vol. 12(1), pp. 3-20.

[4] Barbosa de Freitas, P., Krishnan, V., and Jaric, S., 2007, "Force Coordination in Static Manipulation Tasks: Effects of the Change in Direction and Handedness," Experimental Brain Research, vol. 183(4), pp. 487–497.

[5] Barbosa de Freitas, P., Krishnan, V., and Jaric, S., 2007, "Elaborate force coordination of precision grip could be generalized to bimanual grasping techniques," Neuroscience Letters, vol. 412(2), pp. 179-184.

[6] Barbosa de Freitas, P., Markovic, G., Krishnan, V., and Jaric, S., 2008, "Force Coordination in Static Manipulation: Discerning the Contribution of Muscle Synergies and Cutaneous Afferents," Neuroscience Letters, vol. 434(2), pp. 234–239.

[7] Nayak, A., Khoo, I.-H., Krishnan, V., and Panadda, M., 2018, "Grip Force - Load Force Evaluation and Training Device," M.S. thesis, Department of Electrical Engineering, California State University, Long Beach.

[8] Salarian, A., 2016 "MATLAB Central File Exchange - Intraclass Correlation Coefficient (ICC)," from https://www.mathworks.com/matlabcentral/fileexchange/22099-intraclass-correlation-coefficient-icc.